ISSN 1173-5996

# Predicting Ignition Time Under Transient Heat Flux Using Results from Constant Flux Experiments

**BY**

**Alistair Henderson**

**Supervised by**

**Dr Charley Fleischmann**

**Fire Engineering Research Report 98/4**
**June 1998**

This report was presented as a project report
as part of the M.E. (Fire) degree at the University of Canterbury

School of Engineering
University of Canterbury
Private Bag 4800
Christchurch, New Zealand

Phone 643 364-2250
Fax 643 364-2758

# Abstract

This project investigated if ignition could be mathematically predicted when a material is subjected to a transient heat flux.

Six timbers commonly used in New Zealand for construction and indoor furnishing timbers were tested in a cone calorimeter at the University of Canterbury. The experiments were run at 50, 35, 20 and 15 kW/m2 incident heat flux. The sample surface temperature and heat release data was collected for each test. From the ignition time data a value for thermal inertia was calculated and using specific heat data from the literature the thermal properties of each material was inserted into a One Dimensional Heat Transfer Model.

A second series of tests were conducted on each of the materials tested at constant flux. These new tests involved subjecting the sample to a transient heat flux based on $t^2$ fire growth curves. Again surface temperature and heat release data was obtained from the tests.

The one dimensional heat transfer model was used to attempt to predict the surface temperature profile and the ignition time when the test conditions were entered into it.

It was found that the predicted surface temperature profile generally matched the shape of the measured temperature profile. However the model was unsuccessful in accurately predicting the ignition time in either the constant or transient flux conditions.

It is considered that accurate values for the thermal conductivity and the specific heat would be required before the ignition time and temperature profile could be accurately modelled.

# Acknowledgements

I would first like to thank Dr Charley Fleischmann my supervisor for all of his guidance and suggestions during this year. Both in this project and in the course work.

Thank you to my other lecturer Andy Buchanan, for his support and advice.

Special thanks to Tony Enright for all of his help during the year. I would not have been able to complete the project without your help. I hope I didn't make too much of a pest of myself with all of my questions.

Thanks to Dr Colin Hooker in the Physics Department for all of your help and suggestions in surface temperature measurement.

Thank you to Carol Caldwell and Tony Parkes your suggestions and for reading through what I wrote and critiquing it.

To all of the class this year, thanks for your support and help. I hope the future is all that it promises the class.

Thanks to Ian Sheppard, Mike Flaws and Richard for building everything and helping me when I needed a hand.

Finally, thanks to Mum and Dad, Mark and Oscar for your total support. I wouldn't be here without it.

# Table of Contents

# Table of Figures

# Chapter 1 Introduction

Almost without exception all ignition research has focused on the behaviour of a material when it is exposed to a constant heat flux. Most of this research has focused on ignition as a subsection of Heat Release Rate experiments (therefore the constant flux testing). However in all realistic situations one or all of the following will occur.

- The temperature of the source will alter over time (therefore altering the amount of radiation emitted from the burning object).
- The distance between the radiating object and the receiver decreases (as the flaming area increases or the hot layer descends etc.), thus altering the view factor between the radiator and the receiver.
- The flame height increases, which will have an effect on the amount of radiation emitted from the hot object.

An object that is situated beside a burning object will be subjected to a transient (varying with time) heat flux. Because all past research has concentrated on the behaviour of materials subjected to a constant heat flux, mathematical models have been created to determine ignition behaviour under a transient heat flux.

It is the intention of this project to apply data obtained from constant flux tests in a one dimensional heat transfer model and attempt to predict ignition times firstly for a constant incident heat flux and then for a transient heat flux.

A comparison will then be made with the tests run with a transient incident heat flux.

A secondary problem in New Zealand is that very little research has been performed on local timbers used in the construction industry. In the literature there is a great deal of information on the properties of North American and European timbers, but as these are not used in New Zealand, thermal properties obtained from tests overseas is only loosely applicable. This project aims to obtain information on New Zealand timbers so that this may be used to better understand the behaviour of local timbers.

# Chapter 2 Background Theory and Information

## 2.1 Combustion

Fire is the result of an exothermic chemical reaction between a combustible species and oxygen. A common misconception is that when a material is burning, it is the solid (or liquid) itself that is being consumed in the fire. This is not so. It is in fact gases that are produced by the solid reacting with the oxygen in the surrounding environment that combust and burn. A chemical decomposition process that is called pyrolysis produces these gases. This process occurs in most fuels at elevated temperatures, so that when the fuel is heated there is a point at which the surface layer of the fuel will have become sufficiently hot to start to decompose.

## 2.2 Lower Flammability Limit

Combustion does not occur immediately upon the production of these flammable gases. First there must be a sufficient concentration of the gases at the ignition point for combustion to occur. This minimum concentration of flammable gases in air is called the Lower Flammability Limit (LFL). This must be reached, and there must be sufficient energy in the gases (either through the temperature of the gases or through an external energy source) for ignition to occur (see next section for more complete description of ignition). Reaching the LFL is highly dependent on surrounding environmental conditions. If there is, for example, a significant wind across the surface of the sample, then the combustible gases may be blown away before the minimum concentration can be reached at the ignition source. Therefore a false reading would be given for the ignition time, as the surface would have to be heated to a higher temperature. The higher surface temperature would be required to increase the rate of production of the pyrolyzates to compensate for the gases being 'blown away'. A longer ignition time than that which would be read in calm conditions would result.

## 2.3 Ignition

> *"Ignition may be defined as that process by which a rapid, exothermic reaction is initiated, which then propagates and causes the material involved to undergo change, producing temperatures greatly in excess of ambient"*
>
> Dougal Drysdale, " An Introduction to Fire Dynamics"

When the concentration of the volatile gases produced by pyrolysis reaches the minimum concentration for combustion to occur, it is then possible for ignition to occur. Before ignition can take place several prerequisites must be fulfilled.

- Sufficient quantities of combustible vapours must be emanated as a result of preheating the solid or liquid.
- The combustible gases must have mixed with the oxidant (usually oxygen in the surrounding air).
- There must be sufficient energy supplied for the oxidation reaction to become self accelerative.

In this project ignition is assumed to be a function of the temperature of the fuel and all internal chemistry is ignored..

There are three temperatures that are required to be defined. These are the flashpoint, the firepoint and the autoignition temperature.

The Flashpoint is defined as the lowest temperature at which the fuel/air mixture ignites. This ignition however does not lead to continuous flaming combustion of the fuel as, at this temperature the flow of volatiles from the surface is not sufficient to allow the flame. Therefore once ignition has occurred the volatiles present react with the air and then the flame is extinguished as the concentration of the volatiles drops below the lower flammability limit for the fuel.

The Firepoint is defined as the temperature at which, the flow of volatiles is sufficient to allow flame to persist on the surface of the solid (or liquid). i.e. the temperature of the fuel is sufficient that the flow of volatiles from the fuel surface equals or exceeds the amount of volatiles consumed in combustion.

The Autoignition temperature is defined as the temperature at which the oxidation reaction of the fuel with the air is self-accelerative. This temperature is greater than the fire point for the fuel, so the flow of volatiles is sufficient for combustion. Also the temperature of the fuel surface is sufficient to allow ignition to occur within the boundary layer above the surface of the sample, without the presence of a spark or other ignition source.

In this project the ignition temperature investigated is at the Firepoint. This is to be investigated with the use of a heat release rate cone calorimeter. The ignition source will be an electrical spark above the surface of the sample.

## 2.4 Determining the Thermal Inertia of the Sample

The method used to calculate the thermal inertia of the specimen, as presented by Hopkins[1] uses the following equation to determine the k□c of the sample.

$$k\rho c = \frac{3}{2}\left(\frac{\varepsilon}{slope\left(T_{ig} - T_0\right)}\right) \qquad (2.1)$$

where

| | | |
|---|---|---|
| k | = | Thermal conductivity of the sample |
| ρ | = | Density of the sample |
| c | = | Specific heat |
| ε | = | Emissivity of the sample (assumed to = 1) |
| $T_{ig}$ | = | Ignition temperature of the sample |
| $T_0$ | = | Ambient temperature of surrounding environment |

The slope term in the formula is obtained by calculating the slope of the graph that is obtained when plotting the level of heat flux in the horizontal axis and the inverse of the square root of the time to ignition term on the vertical axis. The plot obtained also has the property of showing the critical heat flux as the intercept with the horizontal axis, (i.e. when the $t_{ig}$ term tends to infinity the $1/\sqrt{(t_{ig})}$ tends to 0).

The density of the sample is measured before the test and the specific heat of the sample is taken as a constant for wood. The value used is presented by Lawson[2] (1952). This allows the calculation of the thermal conductivity of the sample.

A different method of calculating the thermal inertia of the wood samples is given by Janssens[3] (1991). In this method the thermal properties of the wood samples are derived according to the moisture content of the samples.

The calculation of the specific heat and the thermal conductivity of the sample are made according to the following calculations

$$k_{MC} = 0.0237 + \rho_{dry}(2 + 0.247 \times MC) \times 10^{-4} \qquad (2.2)$$

$$c_{MC} = 1200 + \left(\Delta W + L + 4.19 \times \theta_0\right) \times 0.01 \times \frac{MC}{\theta_{ig}} \qquad (2.3)$$

where

$k_{MC}$ = Thermal conductivity of wood at moisture content

$c_{MC}$ = Specific heat of wood at moisture content

$\rho_{dry}$ = density of oven dry wood

MC = Moisture content of wood

$\Delta W$ = Heat of wetting (66.9 kJ $kg^{-1}$)

L = Latent heat of evaporation (2175 kJ $kg^{-1}$)

$\theta_0$ = Temperature rise above ambient to 100°C

$\theta_{ig}$ = $T_{ig} - T_0$

The calculation of the thermal properties from the moisture content of the wood is important for two reasons. The first is that the moisture has an effect on the ignition properties on the wood. The water the is held in the wood at the surface must be evaporated, or driven further into the wood by the heat flux that the sample is exposed to. Thus, if there is a high moisture content, a large amount of the energy is used to overcome the water held in the sample. In a sample with a lower moisture content this energy would be used to raise the temperature of the sample.

The second reason for calculating the thermal conductivity and the specific heat with respect to the moisture content is the values obtained will provide a separate data set of results for comparison.

## 2.5 Modelling a Fire's Heat Release

In this project the method used to calculate the level of incident flux that a sample is exposed to with respect to time is based on a standard $t^2$ fire growth rate. The three standard growth rates are shown in figure 2.1.

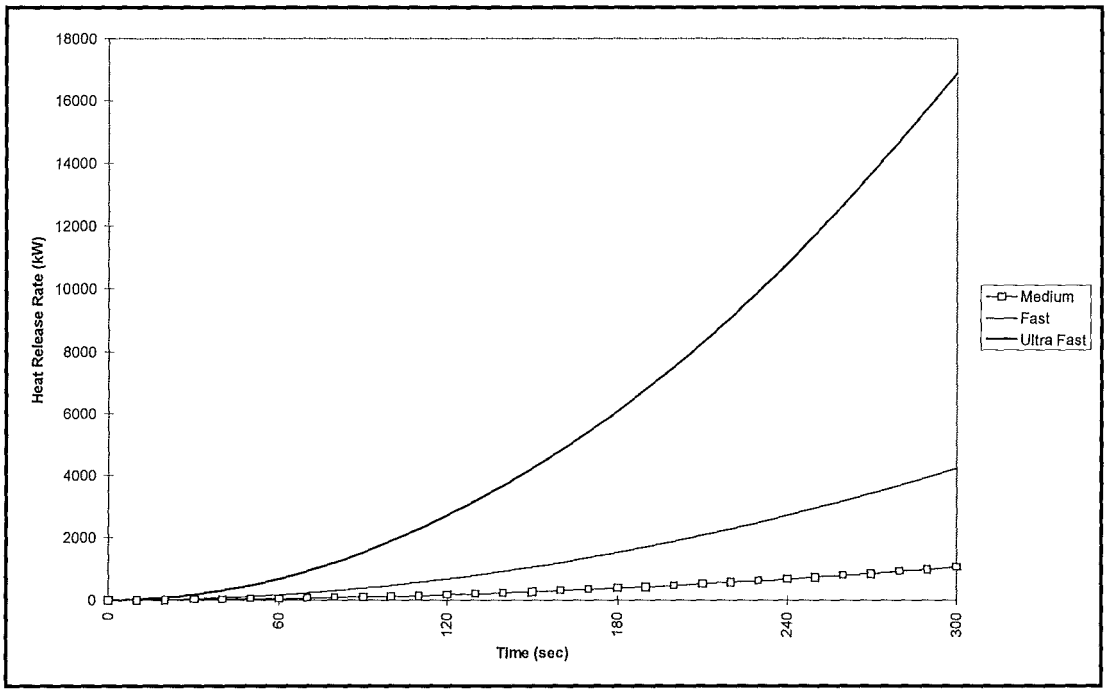


**Figure 2.1 "Heat Release Rates of $t^2$ Fires with Respect to Time"**

As discussed in the cone calorimeter section, because of the limitation of the maximum rate of temperature change being 1°C /second the fire curve that will be modelled is the medium $t^2$ fire.

The received incident radiative flux at the surface of the object calculated with the following equation

$$\dot{Q}_{rec} = Q \varepsilon F_{12} \qquad (2.4)$$

where Q is the heat release rate from the fire

ε is the emissivity

$F_{12}$ is the view factor of the fire from the sample.

The fire characterised by this heat release rate is to be described as a cylinder. The main reason for modelling the fire as specific shape and not as a point source was to attempt to add a sense of a growing fire to the modelled fire. The cylinder, as heat release from the $t^2$ fire increases, will increase in both height and diameter, as a growing fire would. The diameter of the cylinder is described with the relationship

$$Q = q'' A \qquad (2.5)$$

where q" is a constant of the fuel that is being burned representing the heat release rate per meter$^2$. This coefficient has units of kW/m$^2$. The range of values that q" covers is given at 500 - 2500. For this project a value of 1250 kW/m$^2$ is selected.

From the $t^2$ fire growth curve and the above equation it is possible to calculate a fire diameter for a heat release rate. This will determine the size of the 'footprint' of the fire and also determine the distance between the leading edge of the flame and the sample that is receiving the emitted radiation. Since the fire is being modelled as a cylinder the footprint is circular and so the diameter can be obtained from the area.

The other physical aspect of the cylinder that is to be calculated is the cylinder height. Heskestad[4] (1983) derived the following relationship between the heat release rate, the flame diameter and the flame height.

$$L = 0.235Q^{2/5} - 1.02D \qquad (2.6)$$

With these calculations complete the fire that is described by the $t^2$ heat release curve can be described as a physical cylinder with dimensions dependent on the heat release rate.

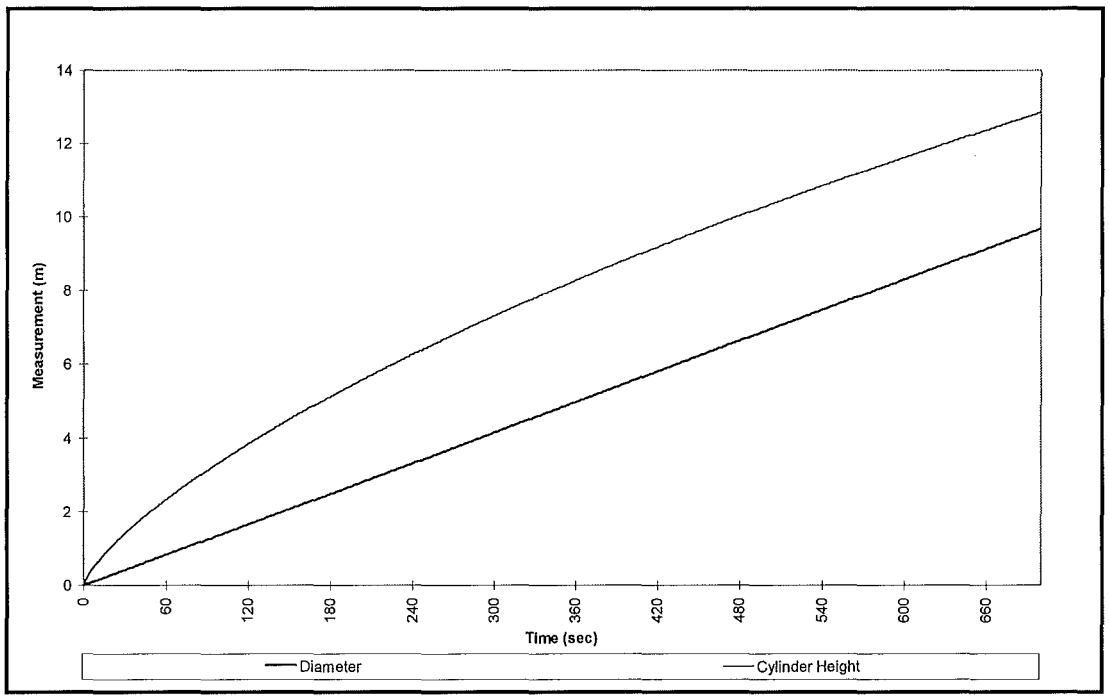


**Figure 2.2 "Plot of Cylinder Height and Diameter Against Time for a Fast $t^2$ Fire"**

The next area that is to be calculated is the view factor between the flame and the sample. In his research Blackshear[4] (1974) developed an expression for the view factor present between a vertical cylinder and vertical square sample with a unit area. This orientation is graphically shown in figure 2.3.

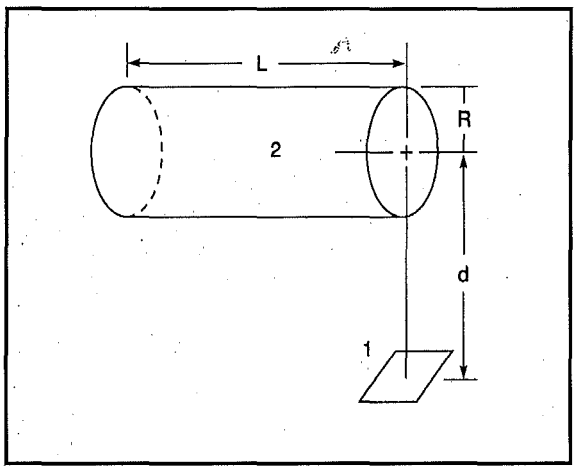


**Figure 2.3 "View Factor Orientation for Cylindrical Flame"**

From this orientation the following relationship for the view factor was calculated.

$$F_{12} = \frac{1}{2\pi}\tan^{-1}\left(\frac{L}{\sqrt{D^2-1}}\right) + \frac{L}{\pi}\left[\frac{A-2D}{D\sqrt{AB}}\tan^{-1}\sqrt{\frac{A(D-1)}{B(D+1)}} - \frac{1}{D}\tan^{-1}\sqrt{\frac{D-1}{D+1}}\right] \quad (2.8)$$

where

$$D = \frac{d}{R} \quad , \quad L = \frac{L}{R} \quad (2.9)$$

and

$$A = (D+1)^2 + L^2 \quad , \quad B = (D-1)^2 + L^2 \quad (2.10)$$

The limiting value for the view factor for this orientation is ½. This means that when the radius of the cylinder approaches the distance between the centre line of the

cylinder and the sample (the flame is about to touch the sample) the view factor approaches ½ asymptotically.

The calculations to derive the view factor were made for a receiver placed a distance of 3.5 m from the vertical centreline of the fire cylinder. This value is the d measurement in equation 2.9.

The last variable that is required for the calculation of the level of heat flux at the receiver is the emissivity of the sample. The emissivity can be defined as the amount of incident radiative energy that an item will absorb. Therefore a sample with an emissivity of 1 will absorb all incident radiative energy, while an item with an emissivity of 0.5 will only absorb ½ of the incident radiative energy, while the remaining portion is transmitted through the sample and reflected from the sample.

The emissivity is calculated with the following equation 2.11

$$\varepsilon = 1 - e^{-D\kappa} \qquad (2.11)$$

where $\kappa$ is the absorption coefficient ($20m^{-1}$)

D is the diameter of the flame.

With the three variables (heat release rate, view factor and emissivity of the sample) it is possible to calculate the incident heat flux at the receiver surface.

Using the Ultra Fast, Fast and Medium $t^2$ fires, the relationship between the heat release rate and the size of the flame 'cylinder', and the view factor calculation the resultant level of incident heat flux calculated at the receiver 3.5 m from the centre of the flame is shown below.

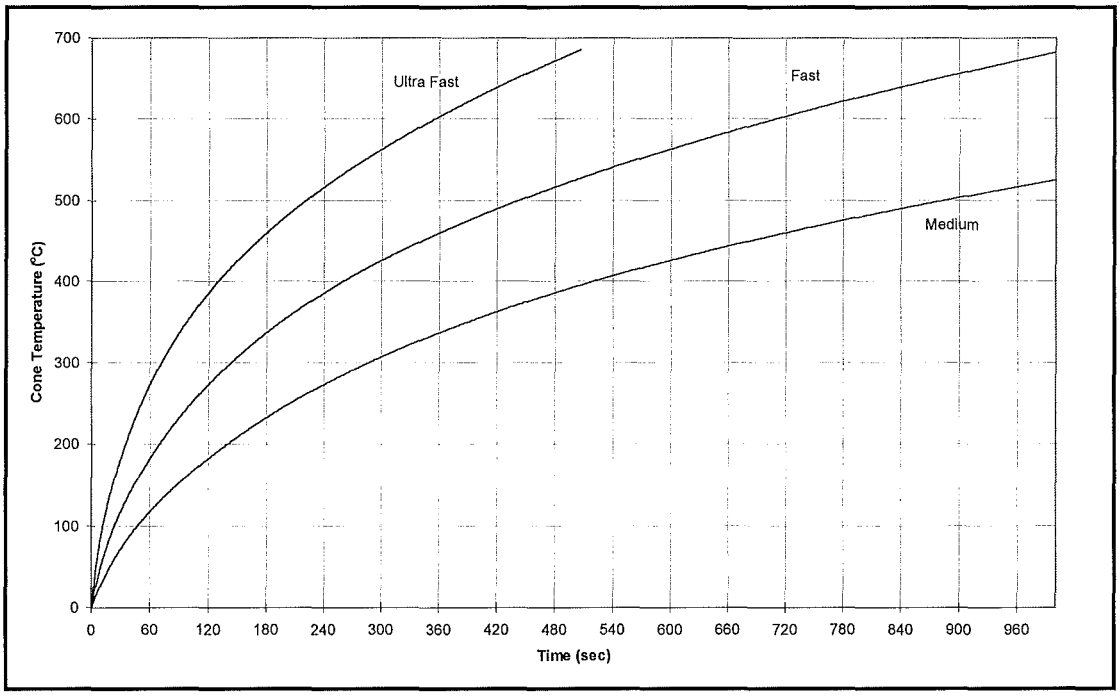


**Figure 2.4: Incident Heat Flux for Ultra Fast, Fast and Medium Fire Growth Curves.**

## *2.6 One Dimensional Heat Transfer Model*

A one dimensional heat transfer model is to be used to predict the ignition times of both constant and transient heat fluxes. Most similar methods used in research have utilised a semi-infinite solid relationship. However with the semi-infinite solid relationship transient boundary conditions can not be applied to the exposed surface. As this project is examining transient conditions this limitation is unacceptable. The model is defined in two parts. The first part deals with the surface temperature of the sample and incorporates the three methods of heat transfer.

- the incident radiation from the cone element
- convection losses from the surface of the sample and
- conduction losses into the sample.

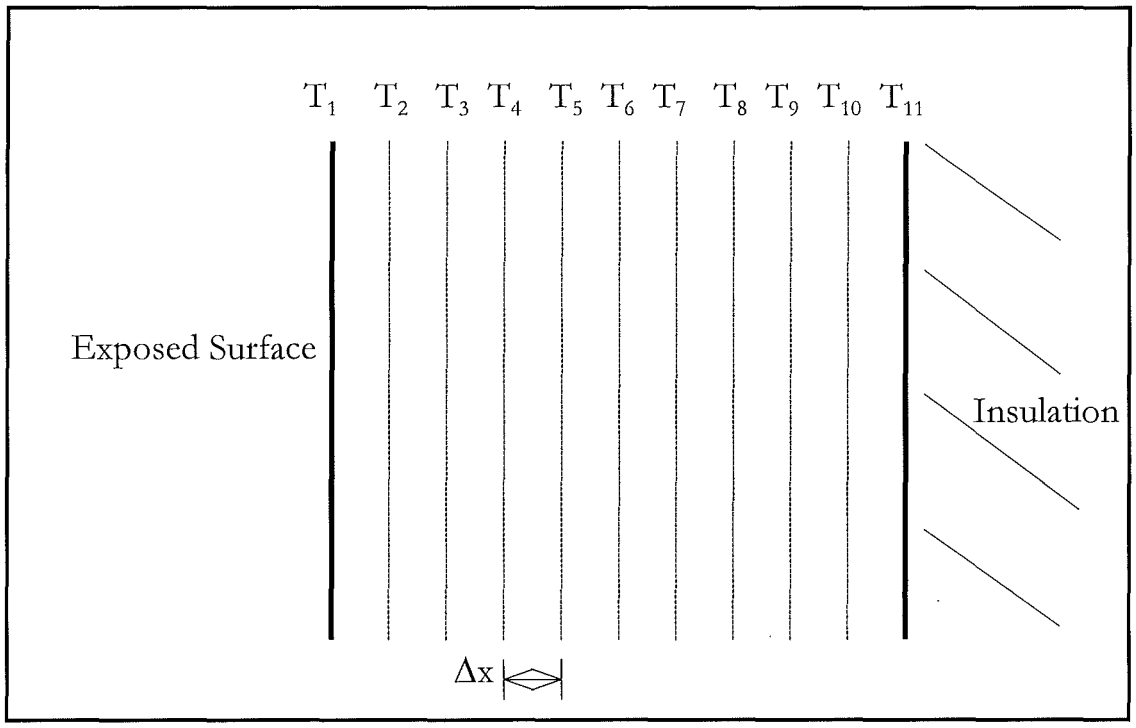


**Figure 2.5: Temperature Points Within Sample For One-Dimensional Heat Transfer Model**

The surface temperature of the sample is determined by:

$$\rho c_p \frac{\partial T}{\partial t} = k \frac{\partial T}{\partial x} + \dot{q}_{rad} + \dot{q}_{conv} + \dot{q}_{inc} \tag{2.12}$$

where

$$\dot{q}_{rad} = \sigma\varepsilon(1 - F_{12})\left(T_\infty^4 - T_1^4\right) \quad \text{radiation losses} \tag{2.13}$$

$$\dot{q}_{conv} = h\left(T_\infty - T_1\right) \quad \text{convection losses} \tag{2.14}$$

$$\dot{q}_{inc} = \sigma\varepsilon F_{12}\left(T_c^4 - T_1^4\right) \quad \text{incident radiation} \tag{2.15}$$

Therefore

$$\frac{\Delta x}{2}\frac{\left[T_1^{t+1} - T_1^t\right]}{\Delta t} = \frac{k}{\rho c_p}\frac{T_2^t - T_1^t}{\Delta x} + \frac{\dot{q}_{rad}}{\rho c_p} + \frac{\dot{q}_{conv}}{\rho c_p} + \frac{\dot{q}_{inc}}{\rho c_p} \tag{2.16}$$

$$T_1^{t+1} - T_1^t = \frac{2\Delta t}{\rho c\ \Delta x}\left[\frac{k}{\Delta x}\left(T_2^t - T_1^t\right) + \sigma\varepsilon\left(1 - F_{12}\right)\left[\left(T_\infty^t\right)^4 - \left(T_1^t\right)^4\right] + h\left(T_\infty - T_1\right) + \sigma\varepsilon F_{12}\left[\left(T_c^t\right)^4 - \left(T_1^t\right)^4\right]\right]$$

$$T_1^{t+1} = T_1^t + \frac{2\Delta t\alpha}{(\Delta x)^2}\left[T_2^t - T_1^t + \frac{\sigma\varepsilon\Delta x}{k}\left[\left(1 - F_{12}\right)\left(T_\infty^t\right)^4 + F_{12}\left(T_c^t\right)^4 - \left(T_1^t\right)^4\right] + \frac{h\Delta x}{k}\left(T_\infty^t - T_1^t\right)\right] \tag{2.17}$$

The second part of the heat transfer model to be defined involves the temperature response within the sample. To achieve this a finite difference approach is used to determine the temperature at nine equally spaced points within the sample.

The finite difference method used in the calculation of the internal temperatures is defined as follows.

$$T_x = \frac{\alpha\Delta t}{\Delta x^2}\left(T_{x-1}^{t-1} + T_{x+1}^{t-1} - 2T_x^{t-1}\right) \tag{2.18}$$

The temperature at the rear surface is determined differently. As there is a layer of insulating material against the rear surface of the sample there is assumed to be an adiabatic boundary in place. This will prevent any heat transfer from the sample to the insulation from occurring.

## 2.8 Oxygen Depletion Calorimetry

Oxygen Depletion Calorimerty is a method of determining the heat release rate of a burning material from the amount of oxygen consumed. It has been found that when organic solids, liquids and gases undergo complete combustion a constant amount of heat is released per unit mass of oxygen consumed (13.1kJ $s^{-1}$).

The method of calculating the heat release rat is detailed in ISO 5660 - Fire Tests - Reaction to Fire Part 1: Heat Release Rate from Building Products (Cone Calorimeter Method)[6].

## 2.9 Measuring the Surface Temperature of the Samples

One of the critical values that needed to be measured is the surface temperature of the samples. As was previously, the surface temperature of the sample at ignition is needed to calculate the thermal inertia of the sample.

The thermocouples used were of Cromal-Alumal type K made of 30 gauge wire. Two sizes of wire were examined for use in measuring the surface temperature. The first was the wire used, as described above. The second was 50 gauge Cromal-Alumal wire. This wire, having such a small mass, does not have the problem of having a significant thermal mass, and therefore does not have a time lag for the wire having to heat up to the temperature of the surroundings. Another advantage of the small wire is that the response of the thermocouple to the direct radiation from the cone heater is negligible due to an extremely small surface area (therefore an extremely small view factor). However the main disadvantage is the size of the wire, in that it is almost impossible to work with accurately. The second problem with the small wire is the weld was created by spot welding the two wires together. The wires were crossed and a capacitor was discharged through them, creating the weld. This has the effect of only fusing the wires at the point that they touched.

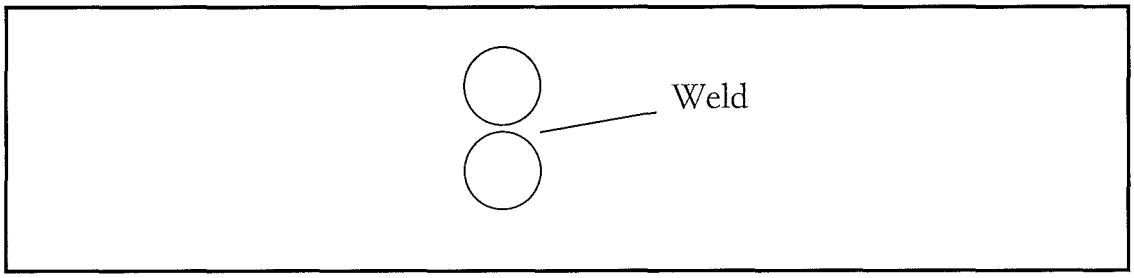


**Figure 2.6: Weld Area in the 50 Gauge Wire Thermocouples.**

Because the fused area is extremely small, the weld is very weak, and so failure often occurred at the weld when mounting the thermocouple on the sample. It is for the reason of the size and the strength that the larger thermocouples were used to measure the surface temperature of the samples.

The larger thermocouples were welded in a different manner. A mercury bath was prepared. (A thick oil layer covered the mercury for safety). This was charged by connecting on terminal of a 80-volt power supply. Both of the thermocouple wires were connected to the other terminal of the supply. By touching the wires to the mercury, the circuit was closed and touching the wires to the mercury melted the wires into a bead.

# Chapter 3 Equipment Used

Two pieces of equipment were used in running experiments. This first is called a "Cone Calorimeter" while the second is an Oxygen Analyser.

## *3.1 Cone Calorimeter*

### 3.1.1 Cone Element

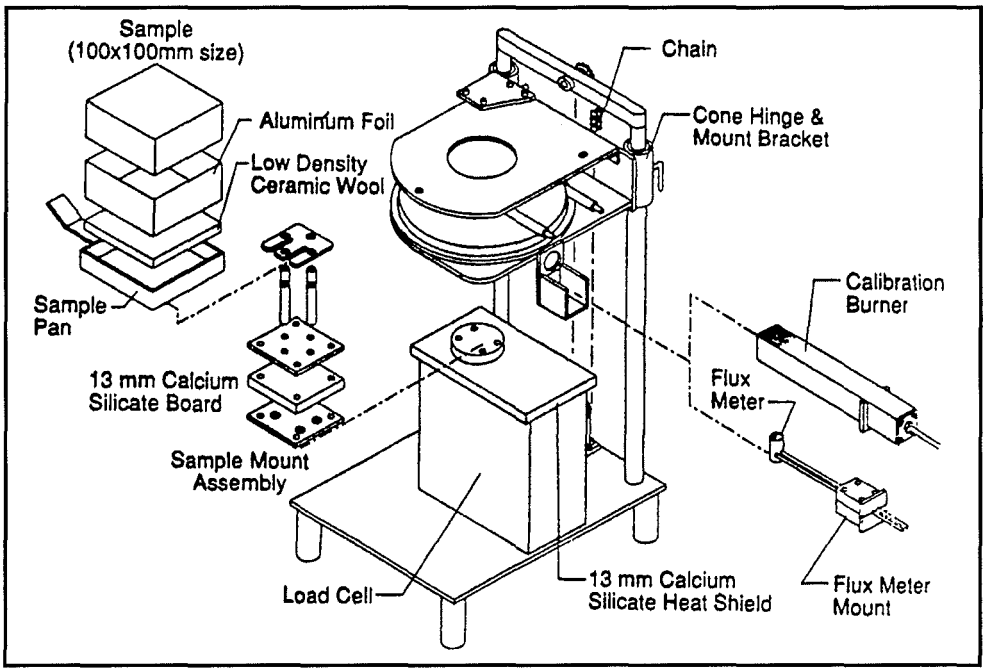


**Figure 3.1: Components of Cone Calorimeter**

Figure 3.1 depicts a typical layout of the cone calorimeter components.

The cone calorimeter derives it's name from the electrical element, which is wound into a truncated cone, used to apply a radiative heat flux onto a sample. Figure 3.2 shows a section view of the cone heater taken through the centre of the element.

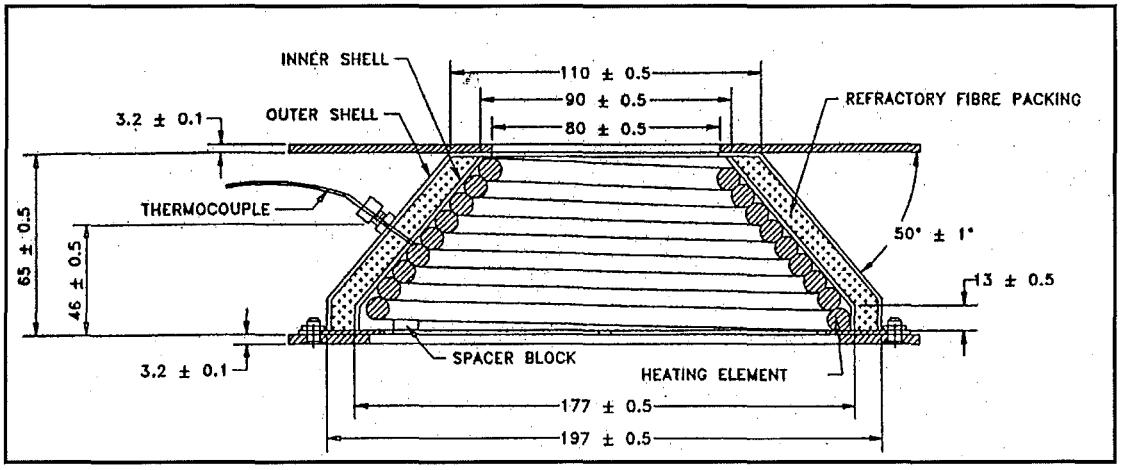


**Figure 3.2: Section Through Cone Heating Element**

The temperature of the cone element is monitored by a set of three thermocouples contacting the coil spaced at equidistant points on the diameter of the cone. The output of these three thermocouples is averaged and the result is displayed on the cone temperature controller display.

### 3.1.2 User Interface

The user interface for the cone calorimeter is primarily through the cone temperature controller. There are two temperatures displayed one above the other on the controller display. The top temperature represents the current cone temperature, while the second value depicts the temperature that the controller has been set to by the operator. The temperature controller has for buttons on the controller panel. The first two are an up and down arrow. These are used to increase or decrease the cone temperature. The remaining buttons are used to vary the characteristics of how the controller functions.

To prevent damage to the cone element through excessive rate thermal expansion, the cone controller is set to a maximum rate of temperature rise of $1^{o}C$ per second.

Other items of interest shown in Figure 3.1 are the Load cell, Flux meter, Calibration burner and the sample.

### 3.1.3 Load Cell

The load cell is responsible for measuring the mass loss rate from the sample during a test. The load cell used in the experiments had a maximum readable loading of 250g, which corresponded to a output voltage of 10V. Before each test the load cell was zeroed with the sample holder on it to make any mass detected on the cell during the test be from the sample.

### 3.1.4 Heat Flux Meter

The flux meter is used to determine the level of heat flux that would be received at the sample surface when the cone is set to a particular temperature. The meter is placed so that the upper surface of cylinder is located 25mm centrally below the lower surface of the cone assembly. Two thermocouples are located at different depths below the exposed surface. Due to various factors such as ageing and sagging of the heater coil, the relationship between heat flux and heater temperature changes with time. Therefore, the aforementioned heat flux calibration has to be repeated frequently. This test was performed prior to each set of tests being performed and the resultant differences between the original calibration runs and the temperature of the cone element was adjusted if necessary.

### 3.1.5 Calibration Burner

The calibration burner is used to calculate the accuracy of the oxygen analyser. The burner is placed so that the upper surface is 25 mm below the lower surface of the cone assembly. In this calibration a quantity of methane is passed through the burner so the flame passes through the cone and into the collection hood.

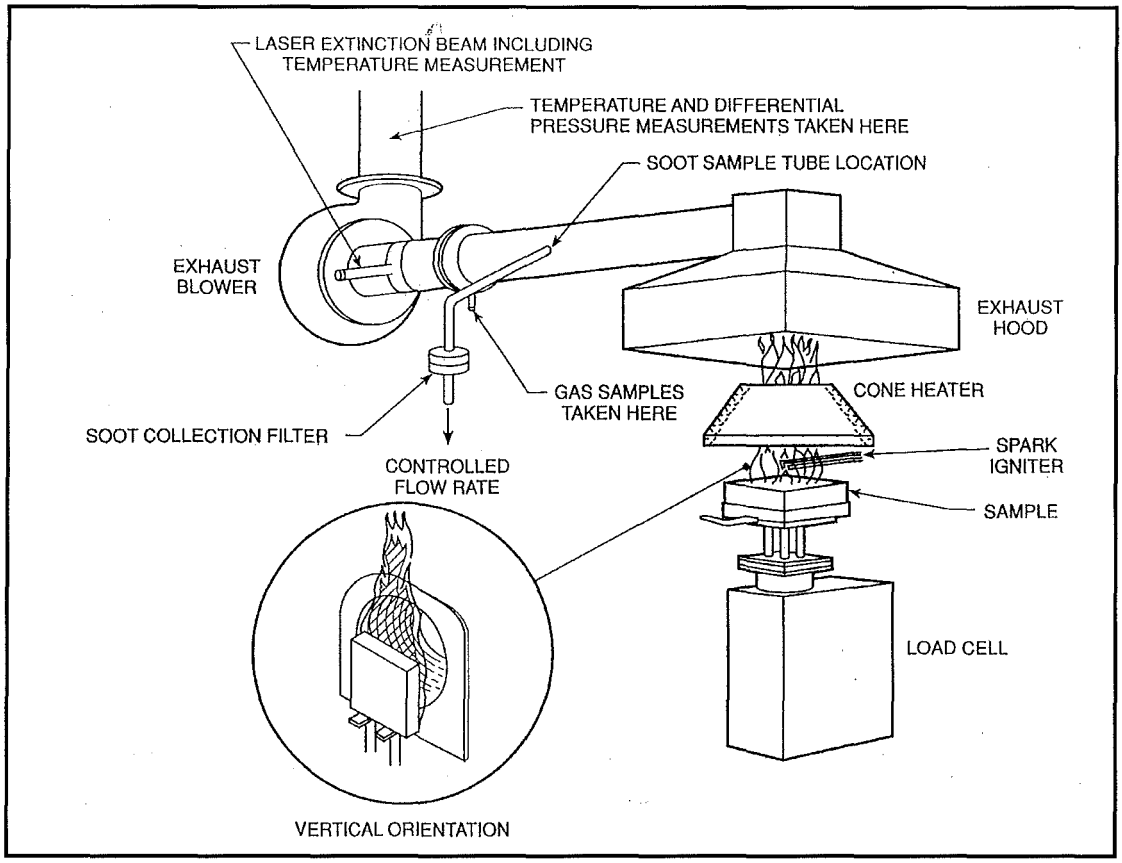


**Figure 3.3: Layout of Cone Calorimeter**

During the calibration burn and during the test, a small quantity of the exhaust gases is extracted from the exhaust flue and is diverted through the oxygen analyser. In figure 3.3 this point is depicted at the point labelled 'Gas Samples Taken Here'.

### 3.1.6 Spark Igniter

Shown in Figure 3.3 is the spark igniter. The device is simply two wires, individually covered in ceramic insulation, with a gap between the two ends over the sample. A capacitor is discharged through the wires several times a second. This discharge creates an electrical arc across the gap. This arc provides the energy necessary to initiate flaming combustion.

For the oxygen analyser to function correctly there must be a constant volumetric flow rate passing the inlet to the analyser. This flow rate is controlled by a centripetal

pump located downstream from the sample port. The flow rate is determined by a pressure probe after the pump.

Thermocouples are attached to the calorimeter at positions indicated on Figure 3.3. An additional thermocouple is attached to the sample surface to determine the surface temperature of the sample during the test.

## *3.2 The Oxygen Analyser*

The oxygen analyser is a device that determines the level of oxygen in the exhaust gases. By analysing this oxygen data the heat release rate from the various samples can be determined.

There are several components in the oxygen analyser set-up. These include a series of filters to remove the particular emissions of the burning object.

- A cold trap consisting of many water chilled glass beads. As the hot extract gases pass over the surface of the beads the water in the flow is condensed out of the gas flow.
- A suction pump to provide the negative pressure within the system to draw the extract gasses from the exhaust flue.
- Containers of silica gel to remove any remaining moisture in the gas flow.
- A container of Calcium Sulphate to remove CO, $CO_2$ from the gas flow.
- The oxygen analyser to determine the level of oxygen in the gas flow.

# Chapter 4 Experimental Methodology

## 4.1 Preparation of Samples

The materials tested in the experimental runs were

- Heart Rimu
- Macracarpa
- Tawa
- Radiata Pine
- MDF
- PMMA

Samples prepared for the tests made were prepared in accordance with the draft ISO 5660 (Fire Tests - Reaction to Fire - Part 1:Heat Release Rate from Building Products (Cone Calorimeter Method)).

Complying with the standard, sample dimensions were 100mm x 100mm, while the depth of the timber samples was

Several variations were made from the standard procedure. Firstly the sampling rate of the data logging equipment was set at 10 samples/second for the constant flux tests and at 8 samples/second for the variable flux tests. Secondly, only one test was performed on the specimens at each heat flux level. The standard calls for three tests at each level of incident heat flux, but for reasons of time limitations and the number of specimens available, only one test was performed on each sample at each heat flux level.

## 4.2 Calibration of the Cone Element of the Cone Calorimeter.

The heat release rate cone calorimeter used in this project first had to be calibrated. By calibrating the cone element the relationship between the temperature of the

element and the level of incident heat flux that is received at the heat flux gauge surface is determined.

The calibration technique involved setting the cone element to temperature points at 50°C steps above 200°C. Each of these temperatures was maintained for 3 minutes to obtain a large data range for the output voltage for each of the temperature points. An average of the output of the gauge voltage readings was taken and this was set as the value of the output voltage for the corresponding temperature. This allows a calculation of a temperature that the cone element needs to be set to achieve an incident heat flux value. Also a trial and error method was used to determine the temperatures that would give an incident heat flux of 15, 20, 35 and 50kW/m$^2$on the gauge's receiving surface.

A daily verification is made of the values obtained by setting the cone element to the constant flux test temperatures and determining the level of incident heat flux that the heat flux gauge is recording.

## *4.3 Preparation and Mounting of the Thermocouples*

The thermocouples were prepared by separating and then shaping the wires around a prepared jig. This gives the shape that allowed the thermocouple to be laid easily on the surface of the sample.

The bead was pressed into the sample surface using a manual bearing press. A steel plate was used to distribute the applied force over the entire upper surface so as to prevent deformation of the wood fibres. To ensure the surface of the sample was not soiled during the pressing operation the surface of the steel plate was cleaned using methylated spirits. Also a sheet of greaseproof paper was laid between the steel and the sample before the thermocouple was pressed into the surface.

The wire was then removed from the surface of the specimen. A small quantity of high temperature glue was used to bond the bead into the depression it made during the pressing process. The thermocouple wire was also formed in a convex curve to

the surface. This would have the effect of making the wire tend to force the bead into the surface. At four sites on the thermocouple wire larger amounts of glue were used to attach the wires to the surface to ensure that the bead was prevented from lifting from the surface during the test.

The PMMA samples were prepared in a slightly different way. By passing a current of 3 Amps through the thermocouple wire the heat generated in the locally heated the surface of the PMMA allowing the thermocouple to be pressed into the surface. It was found during experiments that this method of attaching the thermocouple was not totally effective. When the surface was heated to near the ignition point and the surface started decomposing the surface formed around the thermocouple melted and the thermocouple detached from the surface.

To correct this a small amount of the high temperature glue applied to the wood samples was applied to hold the thermocouple to the surface.

## *4.4 Phase One: Constant Flux Tests*

The first set of tests performed on the samples involved exposing the samples to a constant level of heat flux. The levels of incident heat flux that each of the materials was exposed to was 50, 35, 20 and 15 $kW/m^2$. The procedure for each test is listed below.

Time = 0 seconds
With the data acquisition system running, a baseline was collected for one minute before the sample was exposed to the element.

Time = 90 seconds
The radiation shield above the mass loss sample holder were closed and the sample was inserted into the holder under the heater element.
The surface temperature thermocouple is connected to the system. Care is needed when performing this task as the thermocouple plug must be placed in a suitable

orientation to prevent it from affecting the mass loss data. (The sample is on a load cell that measures the remaining mass of the sample as the test progresses)

Time = 120 seconds
Shutter doors are opened, exposing the sample to the heater element. The spark igniter is inserted immediately after the radiation shield is removed.

Time = 2 minutes - 30 minutes
The following times are recorded.

- Time when flashing or transitory flaming occurs.
- Time when sustained flaming occurs.

Data is collected for 32 minutes after sustained flaming ignition occurs or 30 minutes after the start of the test if ignition has not occurred.

## *4.5 Phase Two : Transient Flux Test*

The transient flux tests were carried out in much the same manner as the constant flux tests. The only difference between the two types of tests is that the cone element temperature is set to a target for a specific time period. The values collected are exactly the same as those that are collected for the constant flux tests.

Because of the 1°C/second temperature rise limitation imposed on the experiments by the cone temperature controller a method of breaking the experiment into separate time steps was implemented. The profile that the cone element must achieve to subject the sample to a simulated $t^2$ fire was broken into time segments of 20 seconds. At the beginning of each time step the cone element temperature controller was set to the temperature that must be achieved in that particular time step. The cone element was then allowed to rise to that temperature at the maximum temperature rise.

For these tests the time to ignition value was obtained with a stopwatch and compared with ignition time given by the data obtained by the surface thermocouple.

After ignition no further increase in the cone element temperature was made and the heat release rate data was collected. Because there is no change in the temperature of the cone element, and therefore the level of heat flux, this heat release data can analysed in the same manner as the constant flux tests.

The temperature profile curves that are used in the transient flux experiments are displayed in 4.1. As noted previously, the rate of temperature rise in the initial period of the test is limited to 1°C/sec.

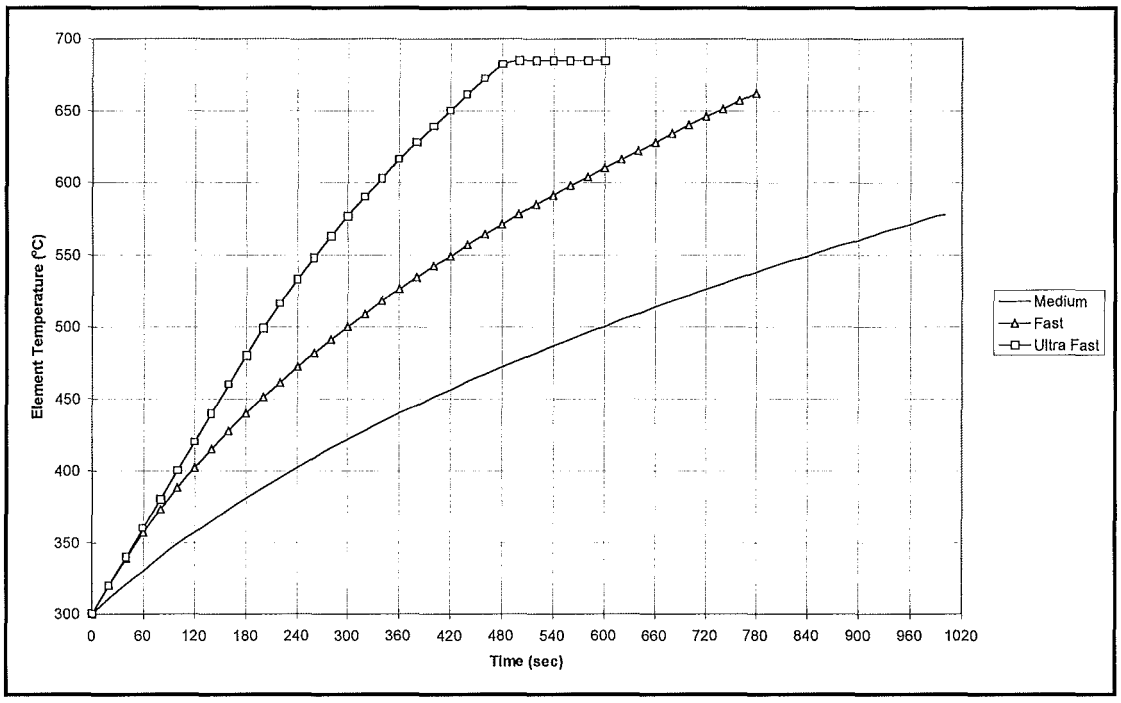


**Figure 4.1: Cone Element Temperature for Ultra Fast, Fast and Medium $t^2$ Fire Growth Curves**

The Ultra Fast cone temperature curve levels off at 480 seconds into the growth. This is because the radius of the fire cylinder has exceeded the 3.5m between the receiver and the centreline of the fire.

# Chapter 5 Data Analysis

## 5.1 Calibrating the Element in the Cone Calorimeter.

The data collected in the cone calorimeter element calibration run is in the form of a plot of the voltage output from the heat flux gauge against time. The voltage output from the gauge is input into a booster device that magnifies the received signal to make reading the output clearly more accurate. The booster device magnifies the input voltage by a factor of 61.61, and has an offset of 3 mV. This offset means that when the input signal is set at 0 mV the output from the booster would read 3 mV.

The data that has been corrected is compared against the calibration graph that was compiled by the manufacturer of the cone calorimeter and the relationship between the temperature of the cone element and the level of incident heat flux at the receiver can be determined.

## 5.2 Analysing Constant Flux Test Data

The critical data that is obtained in the heat flux tests is that which will allow the calculation of the thermal inertia of the material being tested (see Chapter 2 for method of calculating thermal inertia). To obtain this information three values need to be recorded for each test. They are

- The time to ignition of each heat flux level
- The surface temperature of the fuel at ignition
- The ambient temperature during the test

## 5.3 Applying the One Dimensional Heat Transfer Model

The results from the constant flux tests and from the transient flux tests were then compared against the surface temperature curve obtained by inputting the level of incident flux that logged the data acquisition system logged into a one dimensional heat transfer model. This level of incident heat flux is determined by converting the cone temperature into a heat flux. In the transient flux tests this data is critical, as it

determines how closely the actual level of heat flux has followed the theoretical path as determined in Chapter 2.

After the incident heat flux curve is input into the model, the increase in surface temperature will be calculated for each time step. Because ignition is assumed to be a property of the surface temperature in this project this procedure will determine when the surface temperature reaches the ignition temperature for the sample. Thus the time to ignition can be calculated.

With this knowledge the heat transfer model will be used to predict when ignition will occur when a transient flux is applied to the sample. The output of the model will be compared with the experimental result and the accuracy of the model will be determined.

The model will also generate a surface temperature curve for the sample tested. This curve will be compared against the temperature profile that is obtained from the surface thermocouple. This comparison will determine how accurately the heat transfer model predicts not only the time to ignition but how closely the heating of the sample can be predicted.

# Chapter 6 Results and Discussion

For each material tested results collected were used to calculate the heat release rate sample, surface temperature measurements, and the mass loss rate during the test.

## *6.1 Calibration of the Cone Calorimeter.*

The cone calorimeter calibration curve shown in figure 6.1 allows the calculation of the relationship between the temperature that the cone element is set at and the level of incident heat flux.

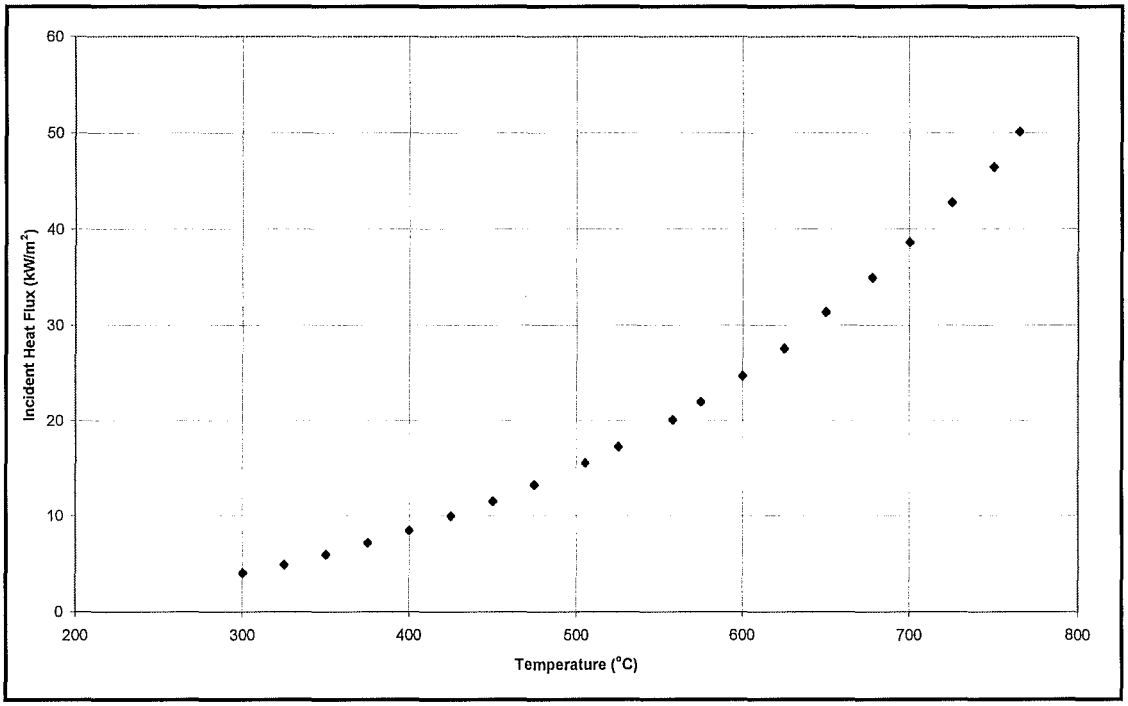


**Figure 6.1: Calibration Curve of the Cone Calorimeter.**

Figure 6.1 represents the first data collected during the project. It is necessary to calculate the temperatures necessary to achieve the required level of heat flux in the constant and the transient flux experiments. The temperature scale that the calibration was taken over represents the range over which runs were made.

## 6.2 Calculating the Thermal Properties of the Materials Tested.

The three ignition variables required from the constant flux tests are

- The level of incident heat flux on the sample.
- The time taken for ignition to occur.
- The surface temperature of the sample at ignition.

The time to ignition values for the different fuels is shown in Table 6.1

**Table 6.1: Time to Ignition in seconds for Fuels Tested at Constant Flux Values.**

| Material ($T_{ig}$ (°C)) | 50 kW/m$^2$ | 35 kW/m$^2$ | 20 kW/m$^2$ | 15 kW/m$^2$ |
|---|---|---|---|---|
| **Tawa (340)** | 42 | 90 | 643 | 1700 |
| **Pine (340)** | 24 | 62 | 345 | 1208 |
| **Rimu (355)** | 31 | 47 | 627 | DNI |
| **Beech (380)** | 31 | 76 | 618 | DNI |
| **Macracarpa (402)** | 25 | 38 | 628 | 1385 |
| **PMMA (345)** | 36 | 57 | 200 | 412 |
| **MDF (330)** | 36 | 62 | 194 | 411 |

The slope of the line fitted to the data is the important piece of information obtained from the modified time to ignition data. From the chart the critical heat flux for the material can be obtained, by calculation the intercept of the line of best fit with the horizontal axis.

The surface temperature of the sample at ignition is determined by correlating the data received from the sample thermocouple with the recorded time to ignition for each of the experimental runs.

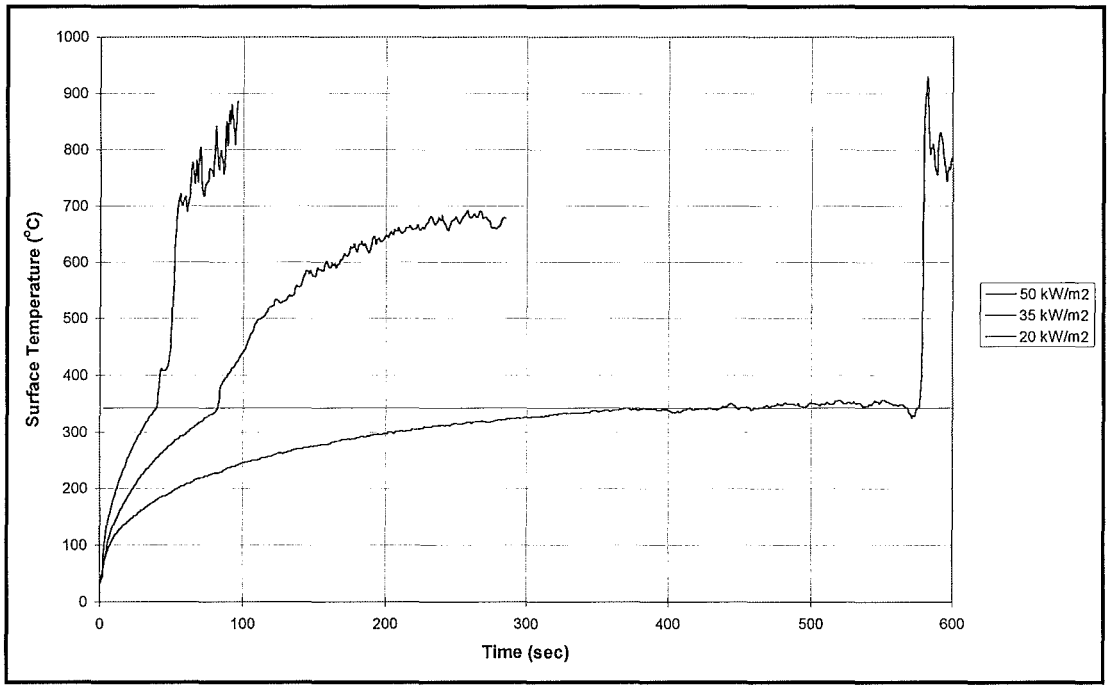


**Figure 6.2: Constant Flux Test Surface Temperature Profiles for Tawa**

The data obtained from the thermocouple imbedded in the surface of the sample gives the recorded temperature profile of the sample surface. From Figure 6.2 the surface temperature of the sample at ignition can be determined. As is displayed in Table 6.1 the surface temperature at which Tawa ignites is 340°C.

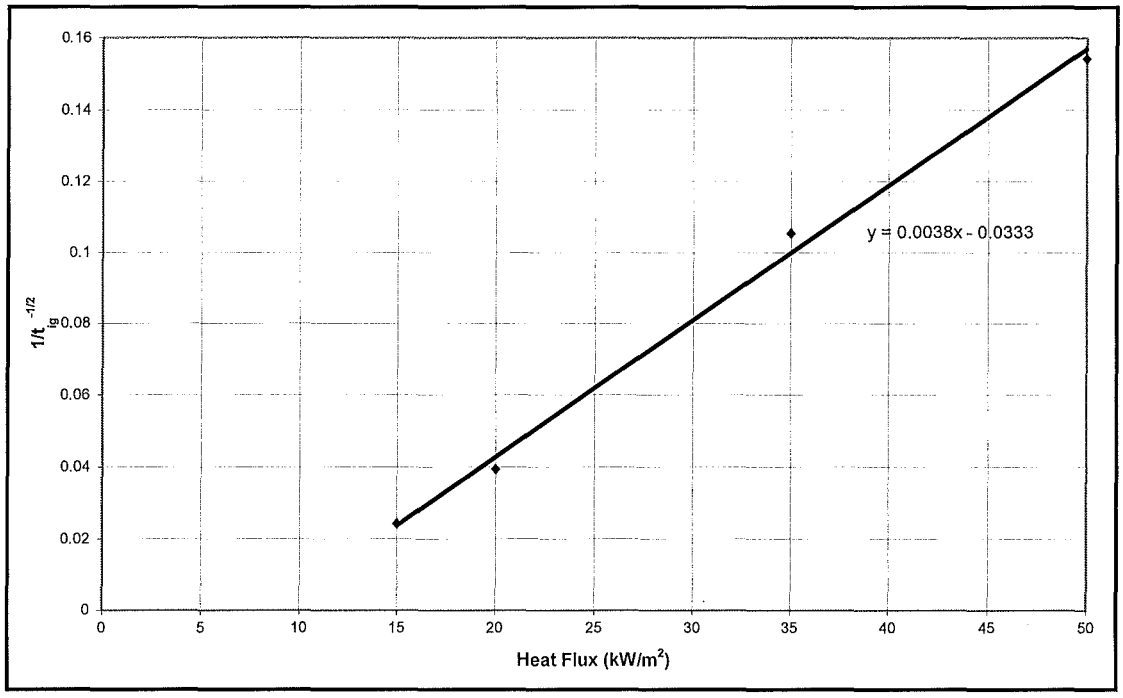


**Figure 6.3: Modified Ignition Data from Constant Flux Tests for Tawa.**

The first calculation made is to determine the thermal inertia 'k□c' of the material. The method described by Hopkins[1] is used for this.

**Table 6.2: Calculation of Thermal Inertia from Ignition Test Results**

| Material | Slope | $T_{ig}$ (°C) | $T_0$ (°C) | kρc ($kJ^2m^{-4}sK^{-2}$) |
|---|---|---|---|---|
| **Tawa** | 0.0038 | 340 | 25.2 | 1.048 |
| **Pine** | 0.0050 | 340 | 22.0 | 0.593 |
| **Rimu** | 0.0050 | 355 | 24.0 | 0.548 |
| **Beech** | 0.0050 | 380 | 20.0 | 0.463 |
| **Macracarpa** | 0.0053 | 402 | 25.0 | 0.376 |
| **PMMA** | 0.0034 | 345 | 20.0 | 1.228 |
| **MDF** | 0.0034 | 330 | 20.0 | 1.377 |

The resultant value for the thermal inertia is used in the calculation of the □ value used in the heat transfer model. The individual values of the thermal conductivity and the specific heat must also be calculated. It has been found by Lawson et al[2] that there is a small variation in the specific heat of wood samples. Using the values for specific heat quoted by Lawson, a value for the thermal conductivity of each sample was calculated (Method One)

Table 6.3: Calculation of the Moisture Content of the Wood

| Material | Mass of Wood (kg) | Mass of Dry Wood (kg) | Moisture Content % |
|---|---|---|---|
| **Tawa** | 0.143 | 0.1282 | 11.54 |
| **Pine** | 0.103 | 0.0925 | 11.35 |
| **Rimu** | 0.132 | 0.1201 | 9.91 |
| **Beech** | 0.0983 | 0.0891 | 9.32 |
| **Macracarpa** | 0.113 | 0.1029 | 10.32 |
| **MDF** | 0.135 | 0.1258 | 7.31 |

The thermal conductivity and the specific heat calculated from the moisture content with Janssens' method (equations 2.2 and 2.3) are displayed in Table 6.4.

Table 6.4: Thermal Properties of Tawa Calculated from the Moisture Content

| Material | k (kW/mK) | ρ ($kg/m^3$) | c (kJ/kgK) |
|---|---|---|---|
| **Tawa** | 0.00033 | 715 | 1.26 |

These values are calculated individually and have no relationship to the thermal inertia calculated previously from the ignition tests. Note that the density has been maintained constant at the measured value.

The value for the specific heat is entered into the k□c value shown in Table 6.2. This gives a second set of values to use in the heat transfer model (Method Two). Finally, the two thermal properties calculated from the moisture content are used in the heat transfer model. (Method Three)

Collating the three different methods of calculating the thermal properties gives the results displayed in table 6.4b. Also presented are the thermal diffusivity values.

**Table 6.4b: Determination of Thermal Properties for Tawa used in One Dimensional Heat Transfer Model.**

| Method of calculating values | k (kW/mK) | ρ ($kg/m^3$) | $c_p$ (kJ/kgK) | α ($m^2/s$) |
|---|---|---|---|---|
| Method 1 | 0.001 | 715 | 1.422 | $9.83x10^{-7}$ |
| Method 2 | 0.0012 | 715 | 1.265 | $1.33x10^{-6}$ |
| Method 3 | 0.00034 | 715 | 1.265 | $3.76x10^{-7}$ |

Table 6.4b shows that there is a large variation in thermal property values used in other research. This is primarily dependent on the thermal conductivity value used. Between two methods of calculating the k value for the *same* material. This disagreement must be resolved before an accurate surface temperature plot may be obtained in a heat transfer model.

## *6.3 Modelling the Surface Temperatures*

### 6.3.1 Phase One: Constant Flux Tests

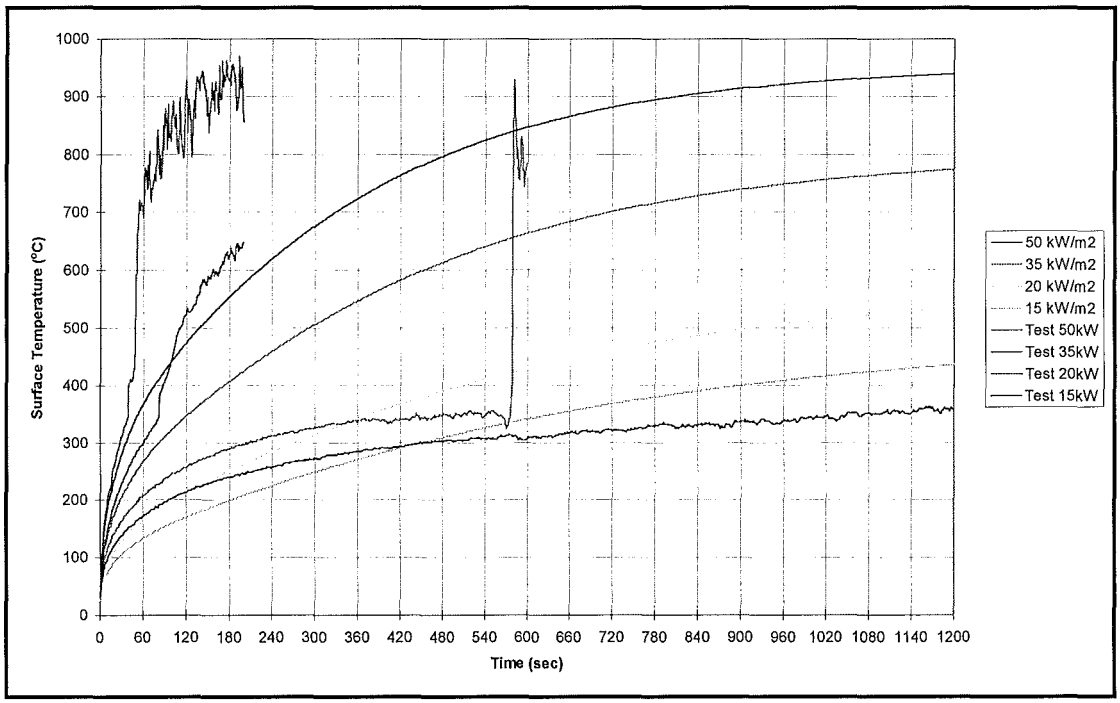


**Figure 6.4: Surface Temperature Profile and Model Output Temperature Curve Using Method One to Calculate the Thermal Properties for Constant Flux Tests.**

The surface temperature profiles depicted in Figures 6.4, 6.5 and 6.6 show that the model output does follow the general temperature profile obtained from the surface thermocouple. The model, while generally following the surface temperature profiles

obtained from the thermocouples is unable to accurately predict when ignition would occur.

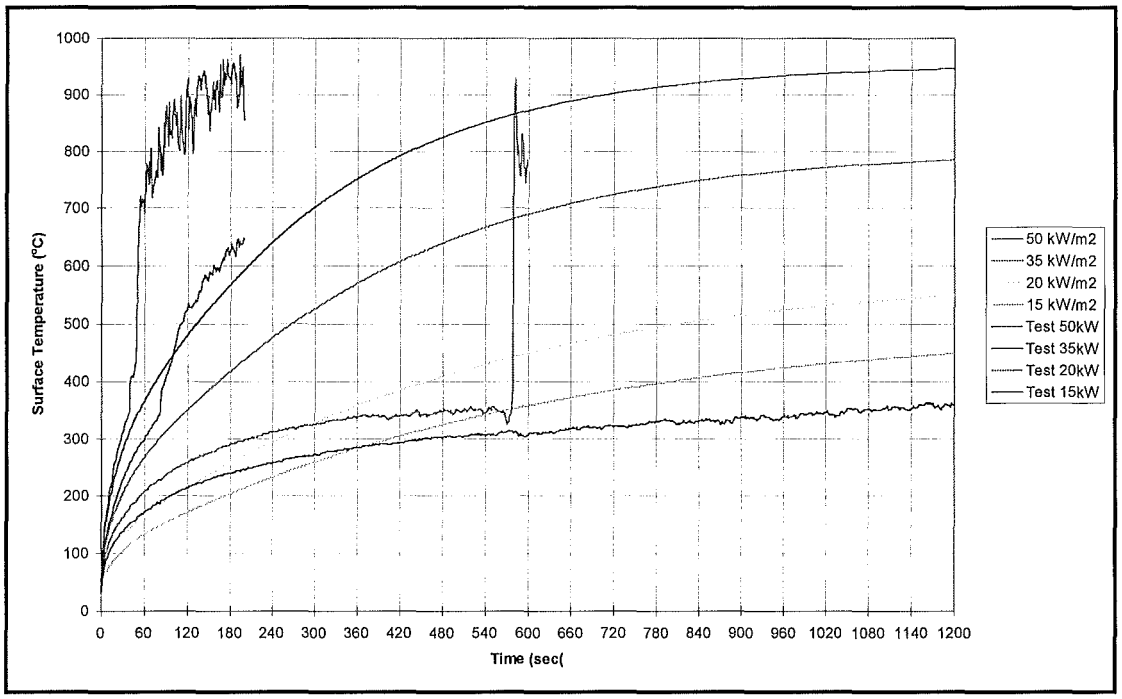


**Figure 6.5: Surface Temperature Profile and Model Output Temperature Curve Using Method Two to Calculate the Thermal Properties for Constant Flux Tests.**

From the three graphs the accuracy of the heat transfer model with respect to the thermocouple temperature curves, is best when at high heat fluxes. This is because of the relatively short ignition times at the higher end heat fluxes

However the general form of the model curves are close to that shown by the thermocouples. The test curves may be reproduced if more accurate values of the thermal conductivity and specific heat are obtained for each individual material.

Figure 6.7 shows in a comparison of the three predicted surface temperature profiles, for 20 kW/m$^2$, that there is significant difference between the predicted temperature profiles for each incident heat flux.

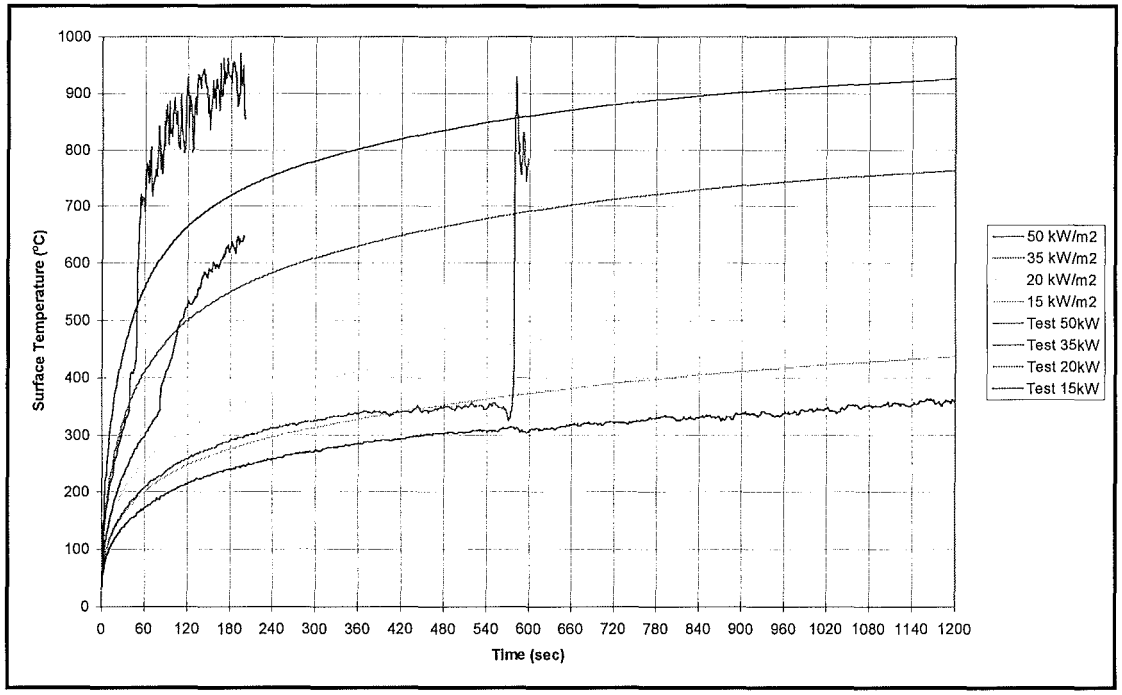


**Figure 6.6: Surface Temperature Profile and Model Output Temperature Curve Using Method Three to Calculate the Thermal Properties for Constant Flux Tests.**

The times to reach the equivalent ignition surface temperature from Figure 6.7 are

- 340 seconds for method one
- 320 seconds for method two
- 160 seconds for method three.

The difference in the surface temperatures is reliant on the Thermal conductivity and specific heat.

This shows that there is a heavy dependence on the thermal properties entered into the heat transfer model. This is expected, as these values are the only values entered into the model to define how a material will behave. From these graphs it is clear that the model is unable to predict accurately the time of ignition.

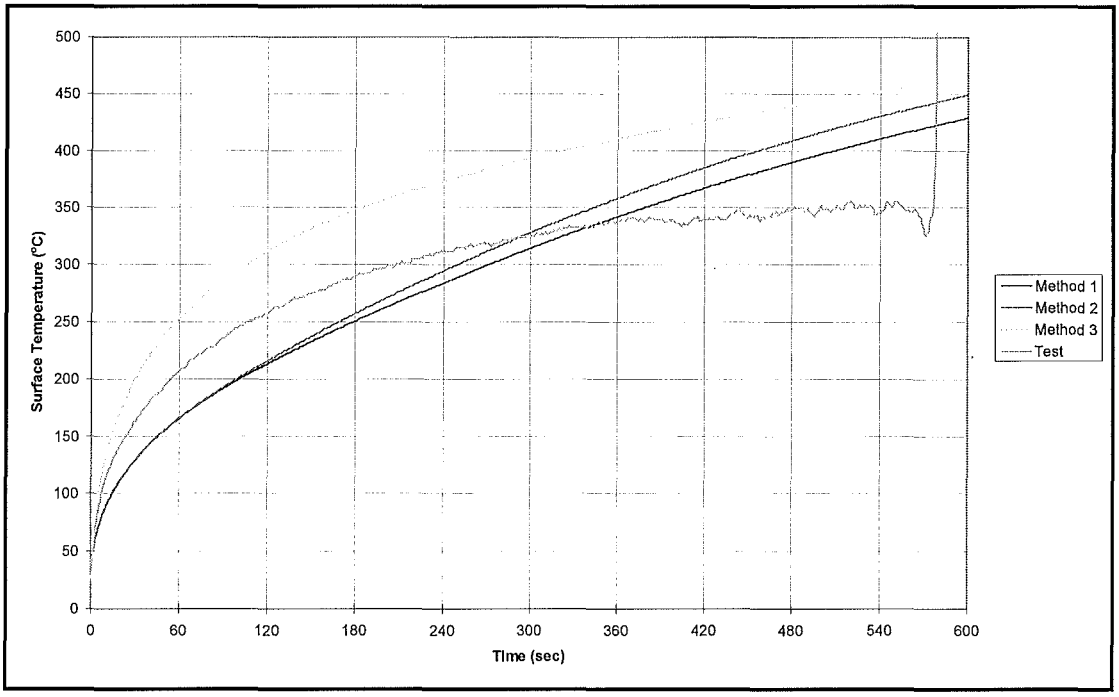


Figure 6.7: Comparison Between the Resultant Output of the Three Methods of Calculating the Thermal Properties and the Measured Temperature Profile for Constant Flux Tests.

### 6.3.2 Phase Two :Transient Flux Tests

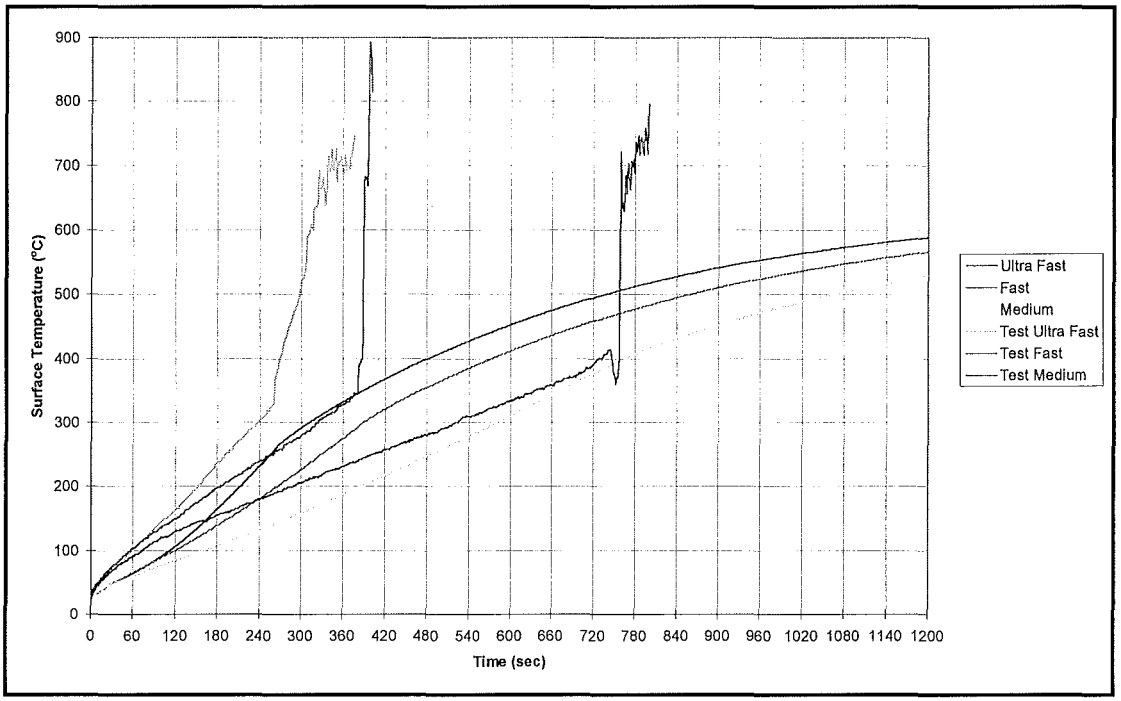


Figure 6.8: Surface Temperature Profile and Model Output Temperature Curve Using Method One to Calculate the Thermal Properties for Transient Flux Tests.

Figures 6.8, 6.9 and 6.10 depict the modelled surface temperature response of the sample to the variable heat fluxes described in Chapter 2.

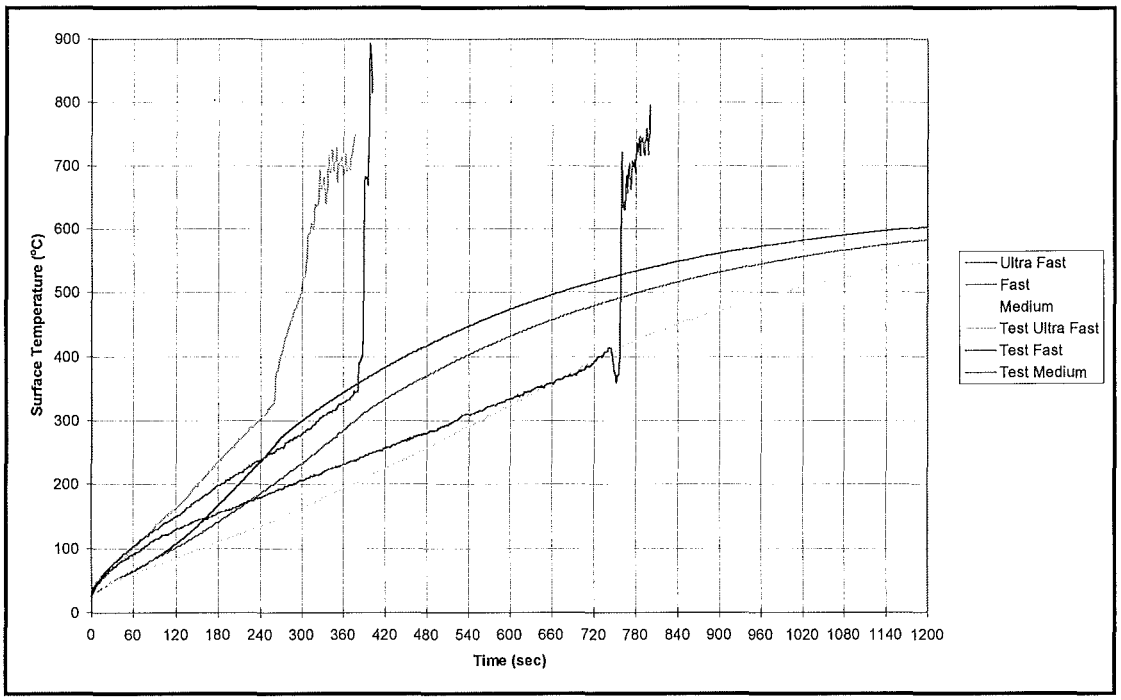


**Figure 6.9 Surface Temperature Profile and Model Output Temperature Curve Using Method Two Calculate the Thermal Properties for Transient Flux Tests.**

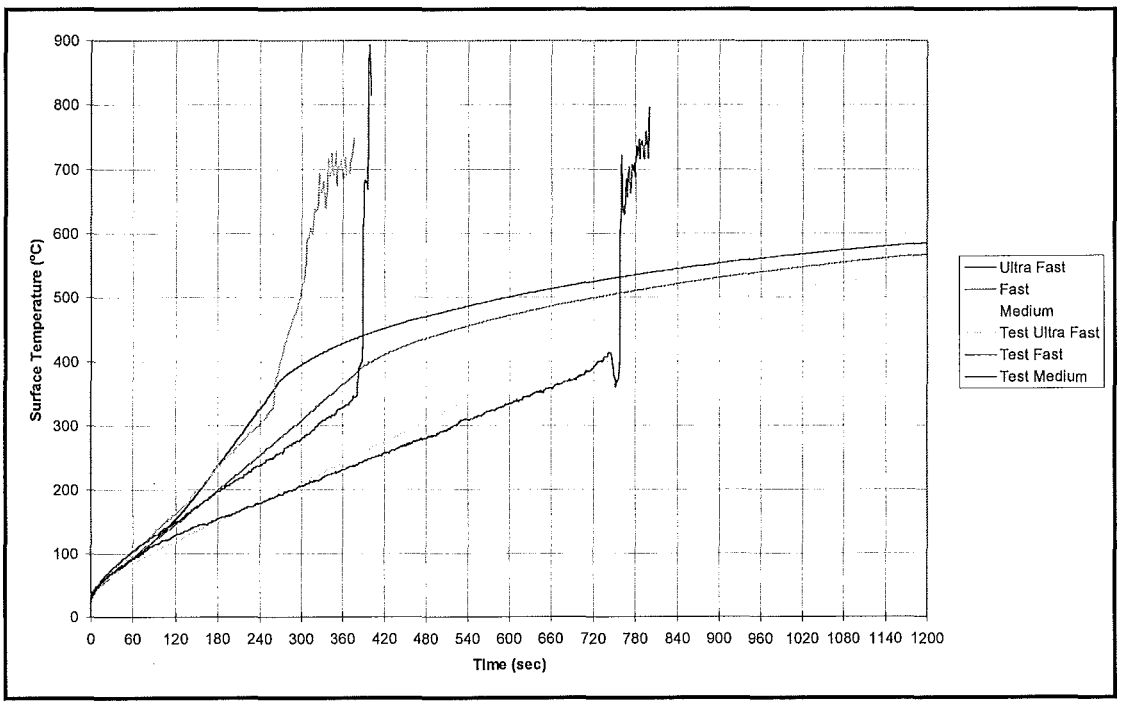


**Figure 6.10 Surface Temperature Profile and Model Output Temperature Curve Using Method Three Calculate the Thermal Properties for Transient Flux Tests.**

In the variable flux tests, as in the heat transfer model output for the three sets of input thermal properties is unable to accurately predict when ignition will occur. Method three is able to most accurately predict when ignition will occur in the variable. The model output with these variables follows the actual fire temperature curves and under predicts the ignition times by

- Ultra Fast: 20 seconds
- Fast: 60 seconds
- Medium: 90 seconds

The temperature profile comparison between the three different methods of calculating the surface temperature give different curves. This is shown in Figure 6.11.

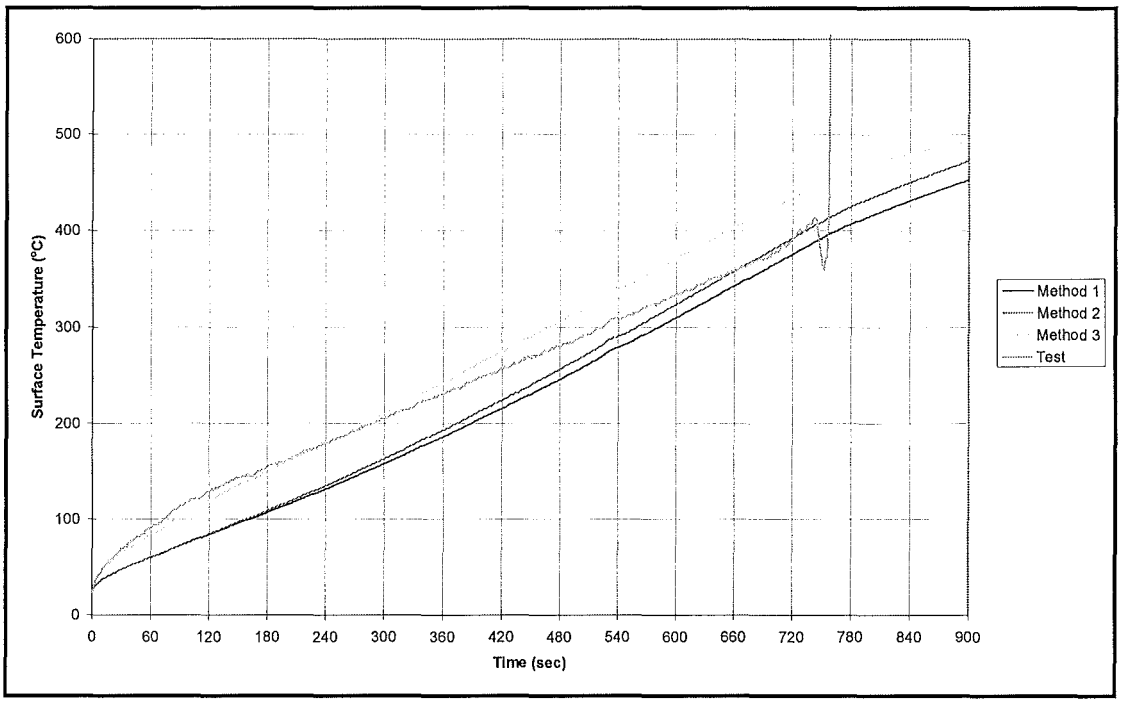


**Figure 6.11: Comparison Between the Resultant Output of the Three Methods of Calculating the Thermal Properties and the Measured Temperature Profile for Transient Flux Tests.**

As discussed in section 6.3.1, the effect that altering thermal properties entered into the heat transfer model has on the predicted temperature profile must be explored further. Obtaining accurate thermal conductivity and specific heat information about

the materials tested would also aid in the prediction of the ignition time of the material when it is exposed to a transient heat flux.

Figure 6.11 shows the measured temperature with the three predicted profiles. The position of the measured profile between the curves of the three calculated methods indicate that a combination of the thermal conductivity and the specific heat may be obtained from continuous simulation, using the three sets of values used in this project as upper and lower limits.

## *6.5 Heat Release Rate.*

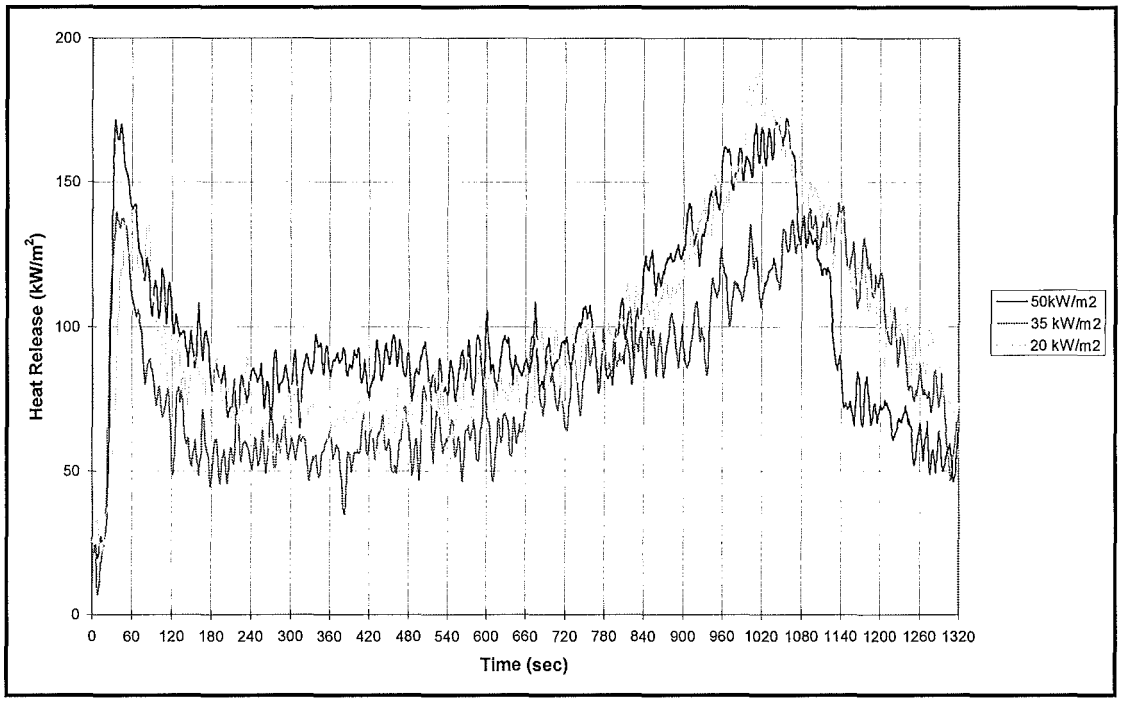


**Figure 6.12: Heat Release Rates for Tawa.**

The heat release characteristics displayed in Figure 6.12 allow the calculation of how much heat the material will emit when it is involved in combustion. This value is called the effective heat of combustion (MJ/kg).

Figure 6.12 shows the plot of the heat release rate over the test period. As can be seen there are two peaks in the data collected. The first peak is due to ignition. Prior to

ignition there is a build up of combustible gases above the surface of the sample. When ignition occurs, these gases are able to combust. These gases are consumed in the combustion reaction and the heat release rate drops to a steady state level.

The second peak is related to the temperature profile through the wood sample. As the temperature within the sample increases , more volatiles are given off. The surface has charred during the test and at the stage where the heat release rate begins to increase, the surface allows the rapid movement of pyrolyzates to the surface reaction zone. Therefore, there is an increase in the mass loss rate as the consumption of fuel increases to maintain the increasing heat release rate. This characteristic is confirmed by Figure 6.13. The mass loss rate increases in conjunction with the increase in the heat release rate.

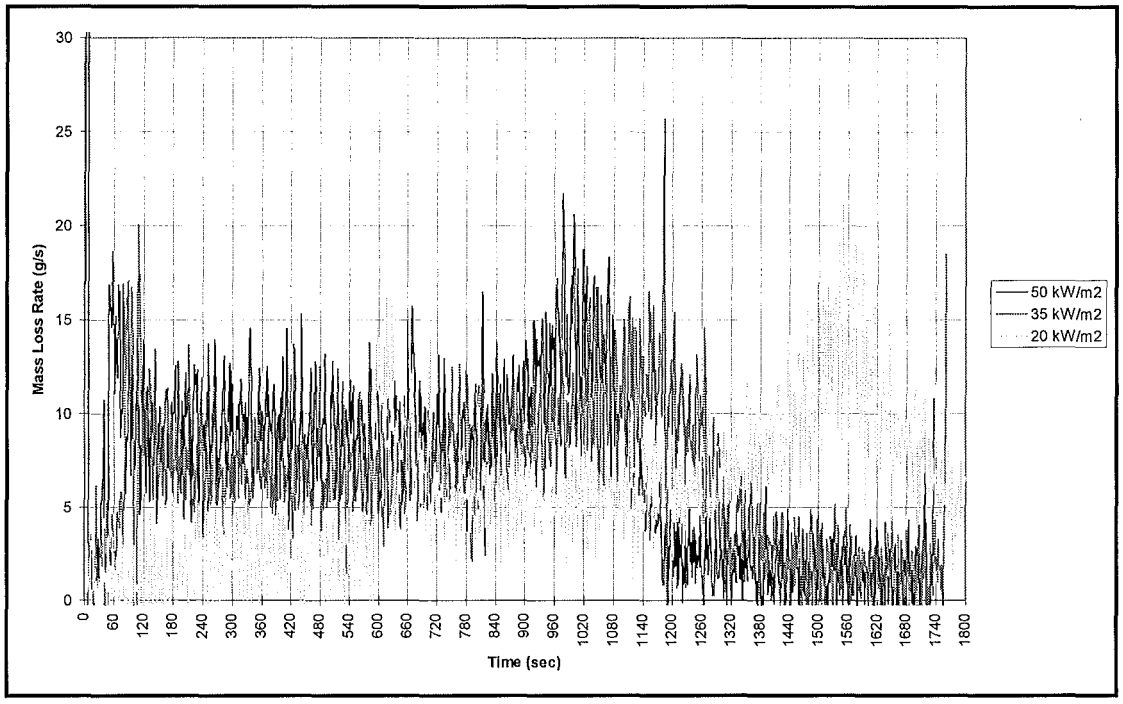


**Figure 6.13: Mass Loss Characteristics for Tawa**

Figure 6.13 shows that after for each test the mass loss rate increases after a period of approximately 600 seconds after ignition. This time corresponds to the beginning of the increase in the heat release rate.

An interesting point occurrence in Figure 6.12 is that the maximum heat release rate for the test at 20 $kW/m^2$ is greater than that for the 50 $kW.m^2$ test. The expected relationship would be that the heat release rate would be greatest for the higher fluxes and would decrease as the level of incident heat flux decreased, as a more intense fast burning fire would be expected at a higher flux level.

# Chapter 7 Testing the Increase from 12kW/m$^2$ to 16 kW/m$^2$ for the BIA Acceptable Solutions

In the New Zealand building industry, the Building Act 1991 is the guiding document that describes the necessary level of protection that a building must have. In the current environment it is possible to satisfy the requirements of this legislation by one of two methods. The first is to design a building to the performance criteria of the Building Act through a "Specific Fire Engineering Solution". The specifics of the fire protection features in the building are irrelevant as long as the performance criteria of the Building Act 1991 are met. The second method of satisfying the Act is to use a set of prescriptive documents called the Acceptable Solutions. If followed, these documents will provide a "socially acceptable" safe level of protection from fire for a building.. At present the maximum allowable level of heat flux that a neighbouring building is to be exposed to is set at 12 kW/m$^2$ in the Acceptable Solutions. This restriction is applicable regardless of the material that the neighbouring building is constructed from, as that building may be removed in the future and a new building constructed with flammable surface materials. However this value is to be raised to 16kW/m$^2$ upon the urging of various elements within the fire protection industry in New Zealand. The raising of the maximum level of incident flux a neighbouring building can be exposed to will have the effect of lowering the level of protection that is required in that building. Another effect would be the allowable the minimum distance between an unprotected building and the neighbouring building to be lowered, resulting in more useful space being available for an unprotected building. These gains would have great financial benefits for the building owner and allow more flexibility when designing the necessary fire protection levels. The question remains however, is it safe?

Piloted ignition was chosen as the method of ignition for this test for the reason that it is the predominant method of ignition in real fire situations. The energy to ignite the gaseous fuel is provided by sparks and other such burning materials from the building

that is on fire. In the tests an electrical spark provided the energy that allowed the materials to ignite at the temperature corresponding to the firepoint.

Heart Rimu, Pine, Tawa, Beech, Macracarpa and Floor MDF were tested at 15 $kW/m^2$. (a lower value than the 16kW/m2 value to be specified in the NZBC. Logic dictates that if the samples tested ignite at 15 $kW/m^2$ then ignition will occur within a shorter exposure period if the specimens were subjected to a 16 $kW/m^2$ incident heat flux.)

It was found that all materials, except Heart Rimu and Beech, ignited when exposed to this level of flux. It can be seen from the surface temperature profile of Beech at 15$kW/m^2$ that the temperature of the surface was approaching the measured ignition time when the test was concluded.

Delichatsios et al[6] has shown that the intercept with the horizontal axis of the plot of heat flux against $t_{ig}^{-½}$ will give a value of 0.7 of the "Critical Heat Flux". This is the minimum heat flux where ignition will occur.

**Table 7.1:Calculation of Critical Heat Flux for Timbers Tested**

| Material | Intercept (kW) | Critical Heat Flux (kW) |
|---|---|---|
| **Tawa** | 8.7 | 12.4 |
| **Pine** | 9.3 | 13.3 |
| **Rimu** | 12.6 | 18 |
| **Beech** | 13.8 | 19 |
| **Macracarpa** | 10.0 | 14.3 |
| **MDF** | 0.9 | 1.3 |

From table 7.1 it is clear that in most cases, if the timber was subjected to the new "safe" limiting heat flux then ignition would occur. The two materials that have critical heat flux values above the 16kW/m2 are those where ignition did not occur for the duration of the test. The values displayed are thought to be suspect.

The conclusion from the tests and the subsequent calculations is that an increase in the minimum safe level of heat flux that a neighbouring property is allowed be exposed to

would be unwise. The tests on the majority of the materials tested show that ignition occurs at a level below this "safe level". Thus it is considered that a neighbouring property would be at risk

# Chapter 8 Anomalies and Sources of Error.

There are several sources of error that have had an effect on the results gained in this project.

The most serious cause of error is the method being used to enter the transient heat flux curves into the temperature controller. Due to the unavailability a computer controller for the temperature setting, the temperatures were input manually at 20 second intervals. This has the effect of relying on the person running the experiment watching a stopwatch and every 20 seconds entering the temperature target for the next 20 second period. This method brings into question the ability to repeat experiments with exactly the same running conditions. However to offset this problem the computer data logger recorded the temperature of the cone element at 1 second time intervals for the duration of the test. Therefore, although the experiments cannot be repeated with absolute accuracy, the heat flux curves that the sample was subjected to during the experiment was entered into the one dimensional heat transfer model.

A primary assumption in the modelling in this project is that ignition is solely a function of the surface temperature. This assumption is neglecting to take into account the chemistry occurring at the surface of the material as it decomposes. It is also neglecting any environmental effects. During the running of the tests that this project is based around, the laboratory, where the tests were being performed, was in the process of being altered with a large extract hood being installed. This created problems with drafts being created when workmen opened doors or cut holes in roofs/walls. Because ignition relies on the concentration of flammable gases to reach a critical level before combustion may occur this intermittent movement of the surrounding air could have had an effect on the data collected.

The method of measuring the surface temperature has introduced a question of the validity of the values obtained. To measure the surface temperature of the sample the thermocouple must be imbedded in the surface. However in the process of imbedding the device in the surface the thermocouple is measuring the temperature of the sample

material approximately ½ mm under the surface of the material. This is the lesser of the problems with the thermocouple. On the surface of the material the bead is exposed to the heat flux imposed on the sample by the cone element. This introduces the problem that the thermocouple will be heated not only by the temperature of the surrounding material, but also by the incident radiation. Therefore the surface temperature values given by the thermocouple are suspect.

A problem that was experienced during the testing program was the data logging computer froze occasionally, usually during a test. This resulted in the loss of any data from that point on. Tests were unable to be repeated due to a lack of time and test specimens. For this reason there are several materials where data has been analysed over a shortened test period than the standard 30 minutes as set down in the standard. This limited time period may also explain the reason why some heat of combustion results calculated are in disagreement.

When calculating the thermal inertia from the slope of the $t_{ig}^{-½}$ against the heat flux a value of zero was entered for the 15kW/m$^2$ entry. This has the effect of increasing the slope of the line of best fit. Also the intercept with the horizontal axis is increased over what would have been recorded had the test been allowed to continue until ignition occurred. The surface temperature profile of the beech at 15kW/m$^2$ clearly shows that the temperature was nearing the point where ignition would occur. This value of zero has the effect of increasing the critical heat flux value calculated from the chart.

In several heat release tests it was found that the heat release from the sample was higher then that at a higher heat flux. This is unexpected, but may be due to a char layer forming on the surface of the sample, therefore insulating the sample. This would cause the temperature within the sample to increase, and therefore the pyrolysis rate would increase. This would produce a greater mass loss rate, which would be converted into a higher heat release rate.

The greatest potential source of error in the heat release calculations, is that only one test was conducted on a sample at each flux level. This is in violation of the standard,

which calls for three tests to be conducted at each level. However for the purposes of this project equipment time limitations prevented this from occurring. Therefore any test where an anomaly occurred has been used to calculate values. If more tests were conducted to verify the results any such error would be detected and allowed for in the analysis.

# Chapter 9 Conclusions

- The One Dimensional Heat Transfer Model can accurately predict the general shape of the surface temperature in response to a constant or transient incident heat flux.

- The thermal properties of the material are of critical importance to the predicting of the ignition time with a heat transfer model. Accurate values need to be established before attempting to model ignition time accurately.

- The increase of the minimum *safe* level of heat flux a neighbouring building will be exposed to from a fire from 12 kW/m2 to 16kW/m2 is not recommended. Timber materials commonly used in constructing exterior surfaces of buildings ignited at levels of heat flux below that which is proposed.

# Chapter 10 Further Research

There is a great amount of further work to be completed on this topic. Some suggestions to move on from this project are

- Further ignition testing of New Zealand timbers to confirm ignition results obtained.

- Further Heat Release Rate tests to be made on the timbers tested, to verify or correct the values obtained.

- Testing of New Zealand timbers to obtain a set of accurate thermal property values, and therefore enter these into the heat transfer model and attempt to predict the ignition time.

- Further investigation into temperature curves obtained and attempt to modify the thermal values used within boundaries of values used in this project to attempt to make model predicted surface temperature curve follow the measured temperature curves.

# Chapter 11 References

1. Hopkins D (Jr), "Predicting the ignition time and Burning rate of Thermoplastics in the cone calorimeter", NIST-GCR-95-677 (1995)

2. Lawson D.I, Simms D.L, "The Ignition of Wood by Radiation", *British Journal of Applied Physics*, vol **3**, No 9, (1952)

3. Janssens M.L, Fundamental Thermophysical Characteristics of Wood and their Role in Enclosure Fire Growth" PhD Thesis, University of Gent (1991)

4. SFPE Handbook of Fire Protection Engineering, Section 2, Chapter 2.

5. Blackshear P, "Heat Transfer in Fires: Thermophysics, Social Aspects, Economic Impact", (1974).

6. International Standard ISO 5660 - Fire Tests-Reaction to Fire Part 1:Heat Release Rate from Building Products (Cone Calorimeter Method)

7. Delichatsios M.A, Panagioyou TH, Kiley F, "The use of Time to Ignition Data for Characterising the Thermal Inertia and the Minimum (Critical) Heat Flux for Ignition or Pyrolysis, *Combustion and Flame*, 84 (1991)

# Chapter 12 Bibliography

Atreya A, Mahmood A, "Effect of Environmental Variables on Piloted Ignition, *Fire Safety Science - Proceedings of the Third International Symposium.*

Babrauskas V., "Ten Years of Heat Release Research with the Cone Calorimeter", Heat Release and Fire Hazard, Vol. I, Y. Hasemi, ed., Building Research Institute, Tsukuba, Japan (1993).

Babrauskas V., Parker W, "Ignitability Measurements with the Cone Calorimeter", *Fire and Materials*, **11**, (1987)

Blackshear P.L, "Heat Transfer in Fires : Thermophysics, social aspects, economic aspects", John Wiley & Sons (1974)

Deepak D, Drysdale D.D, "Flammability of Solids: An Apparatus to Measure the Critical Mass Flux at the FirePoint", *Fire Safety Journal*, **5** (1983)

Delichatsios M.A, Panagioyou TH, Kiley F, "The use of Time to Ignition Data for Characterising the Thermal Inertia and the Minimum (Critical) Heat Flux for Ignition or Pyrolysis, *Combustion and Flame*, 84 (1991)

Drysdale D.D, Thomson H.E, "Flammability of Plastics I : Ignition Temperatures", *Fire and Materials*, **2** ( 1987 )

Drysdale D.D, Thomson H.E, "Flammability of Plastics II : Critical Mass Flux at the Firepoint", *Fire Safety Journal*, **14** ( 1989 )

Fangrat J, Hasemi Y, Yashida M, Hirata T, "Surface Temperature at Ignition of Wooden Based Slabs", *Fire Safety Journal*, **29** (1996)

Gardner W.D, Thomson C.R, "Ignitability and Heat Release Properties of Forest Products", *Fire and Materials*, **15** (1991)

Hanaizumi H, Toyota H, "High Accuracy Measurements of Emisivity and Temperature of Various Materials near 300K Using a Radiomater with 5 mK Temperature Resolution", *Temperature: Its Measurement and Control in Science and Industry*, A.I.P, vol **6**, Part 2.

Hao T.C, White R.H, "Burning Rate of Solid Wood Measured in a Heat Release Rate Calorimeter", *Fire and Materials*, **16** (1992)

International Standard ISO 5660 - Fire Tests-Reaction to Fire Part 1:Heat Release Rate from Building Products (Cone Calorimeter Method)

Janssens M.L, Fundamental Thermophysical Characteristics of Wood and their Role in Enclosure Fire Growth" PhD Thesis, University of Gent (1991)

Janssens M.L, "Piloted Ignition of Wood: A Review", Fire and Materials, **15**, (1991)

Janssens M.L, "A Thermal Model for Piloted Ignition of Wood Including Variable Thermophysical Properties", Fire Safety Science - Proceedings of the Third International Symposium.

Kanury A.M, "Ignition of Cellulosic Solids-A Review", Fire Research : Reviews and Abstracts.

Kashiwagi T, "A Radiative Ignition Model of a Solid Fuel", *Combustion Science and Technology*, vol **8** (1974)

Kashiwagi. T, "Effects of Sample Orientation on Radiative Ignition", *Combustion and Flame*,

Kashiwagi. T, "Radiative Ignition Mechanism of Solid Fuels", *Fire Safety Journal*, **3** (1981)

Lawson D.I, Simms D.L, "The Ignition of Wood by Radiation", *British Journal of Applied Physics*, vol **3**, No 9, (1952)

Martin S, "Diffusion-Controlled Ignition of Cellulosic Materials by Intense Radiant Energy", *Tenth Symposium (International) on Combustion* (1965)

McGuire J.H, "Limited Safe Surface Temperatures for Combustible Materials" National Research Council of Canada (1969)

Moysey E.B, Muir W.E, "Pilot Ignition of Building Materials by Radiation", *Fire Technology*, (Unknown Edition Number or Date)

Niioka T, Williams F.A, "Relationship between theory and Experiment for Radiant Ignition of Solids", *17th Symposium (International) on Combustion.*

Scudamore M.J, Briggs P.J, Prager F.H, "Cone Calorimetry - A Review of Tests Carried out on Plastics for the Association of Plastic Manufacturers of Europe", *Fire and Materials*, **15** (1991)

SFPE Handbook of Fire Protection Engineering, 2nd edition
Shields T.J, Silcock G.W, Murray J.J, "Evaluating Ignition Data Using the Flux Time Product", *Fire and Materials*, **18** ( 1994 )

Silcock G, Shields, T, "A Protocol for Analysis of Time-to-Ignition Data From Bench Scale Tests", *Fire Safety Journal*, **24**, (1995)

Simms D, Law M, "The Ignition of Wet and Dry Wood by Radiation", *Combustion and Flame*, vol **11**, No 5, (1967)

Tewarson A, "Flammability Parameters of Materials : Ignition, Combustion, and Fire Propagation", *Journal of Fire Sciences*, vol **12** (1994)

Thomson H.E, Drysdale D.D, Beyler C.L, "An Experimental Evaluation of Critical Surface Temperature as a Criterion for Piloted Ignition of Solid Fuels", *Fire Safety Journal*, **13** (1988)

Thomson H.E, Drysdale D.D, "Flammability of Plastics 1: Ignition Temperatures", *Fire and Materials*, **11** (1987)

Toal B.R, Silcock G.W.H, Shields, T.J, "An Examination of piloted Ignition Characteristics of Cellulosic Materials Using the ISO Ignitability Test", *Fire and Materials* , **14** ( 1989 )

Tran H.C, White R.H, "Burning Rate of Solid Wood Measured in a Heat Release Rate Calorimeter", *Fire and Materials*, **16** (1992)

Tran H.C, White R.H, "Burning Rate of Solid Wood Measured in a Heat Release Rate Calorimeter", *Fire and Materials*, **16** (1992)

Weatherford W.D Jr, Sheppard D.M, Basic Studies of the Mechanism of Ignition of Cellulosic Materials, *Tenth Symposium (International) on Combustion* (1965)

Whiteley R.R, "Some Comments on the Measurement of Ignitability and on the Calculation of 'Critical Heat Flux'", *Fire Safety Journal*, **21** (1993)

# Chapter 13 Appendices

# Appendix A : Rimu

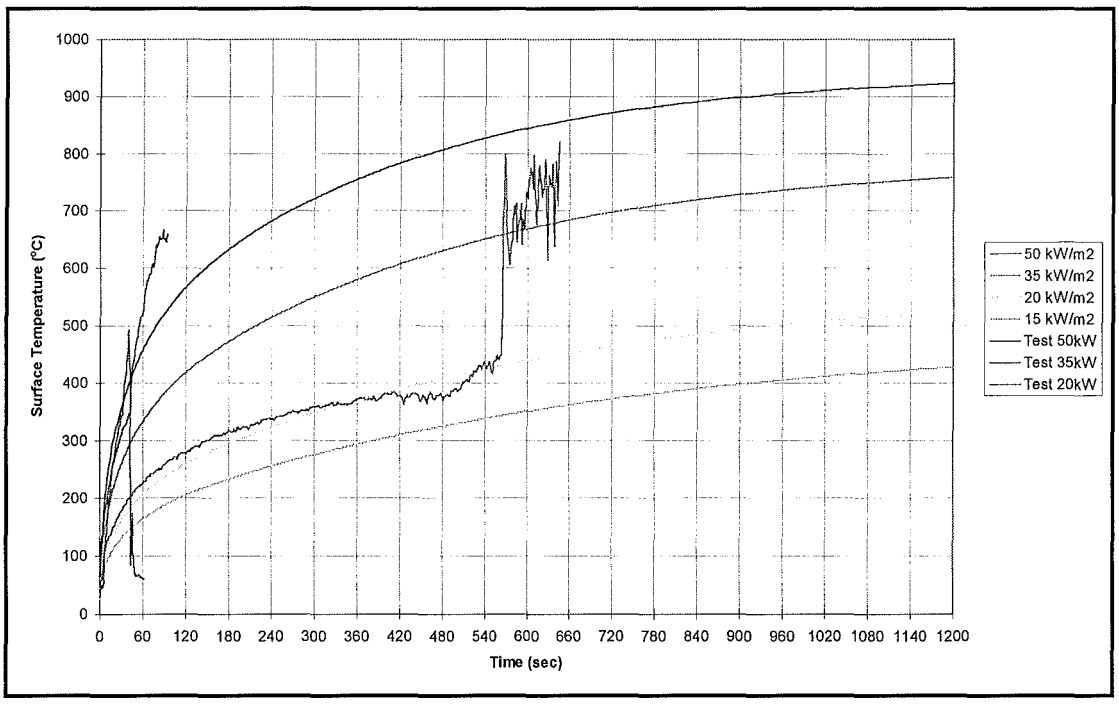


Surface Temperature Profile and Model Output Temperature Curve Using Method One to Calculate the Thermal Properties for Constant Flux Tests.

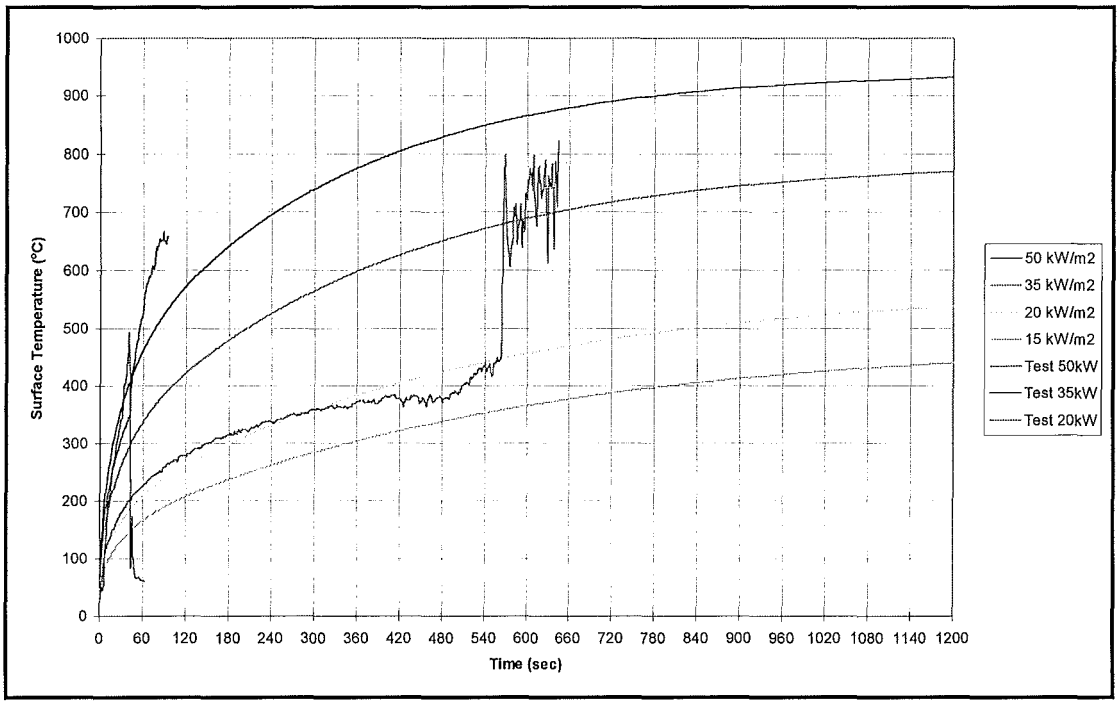


Surface Temperature Profile and Model Output Temperature Curve Using Method Two to Calculate the Thermal Properties for Constant Flux Tests.

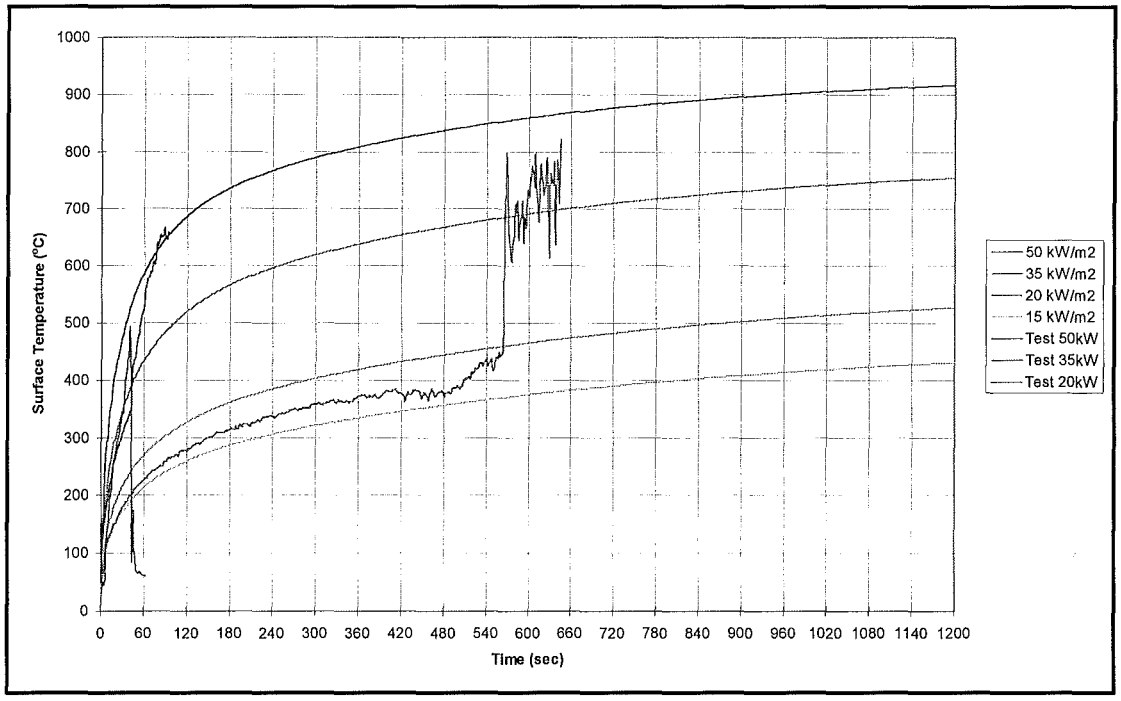


**Surface Temperature Profile and Model Output Temperature Curve Using Method Three to Calculate the Thermal Properties for Constant Flux Tests.**

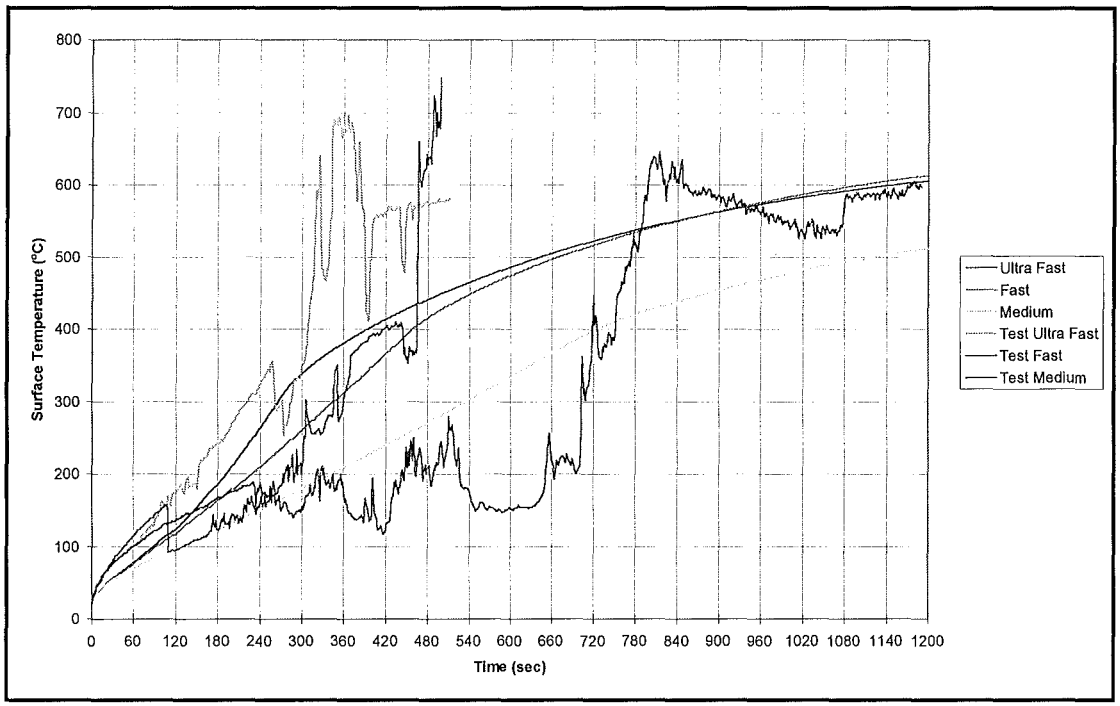


**Surface Temperature Profile and Model Output Temperature Curve Using Method One to Calculate the Thermal Properties for Transient Flux Tests.**

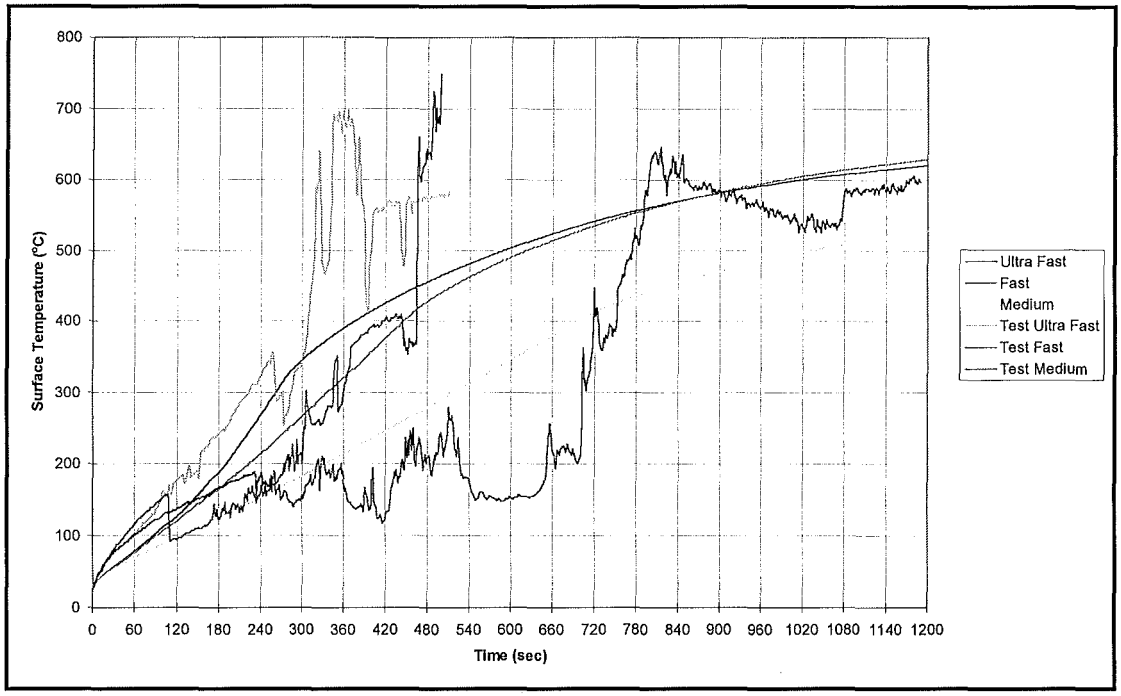


**Surface Temperature Profile and Model Output Temperature Curve Using Method Two to Calculate the Thermal Properties for Transient Flux Tests.**

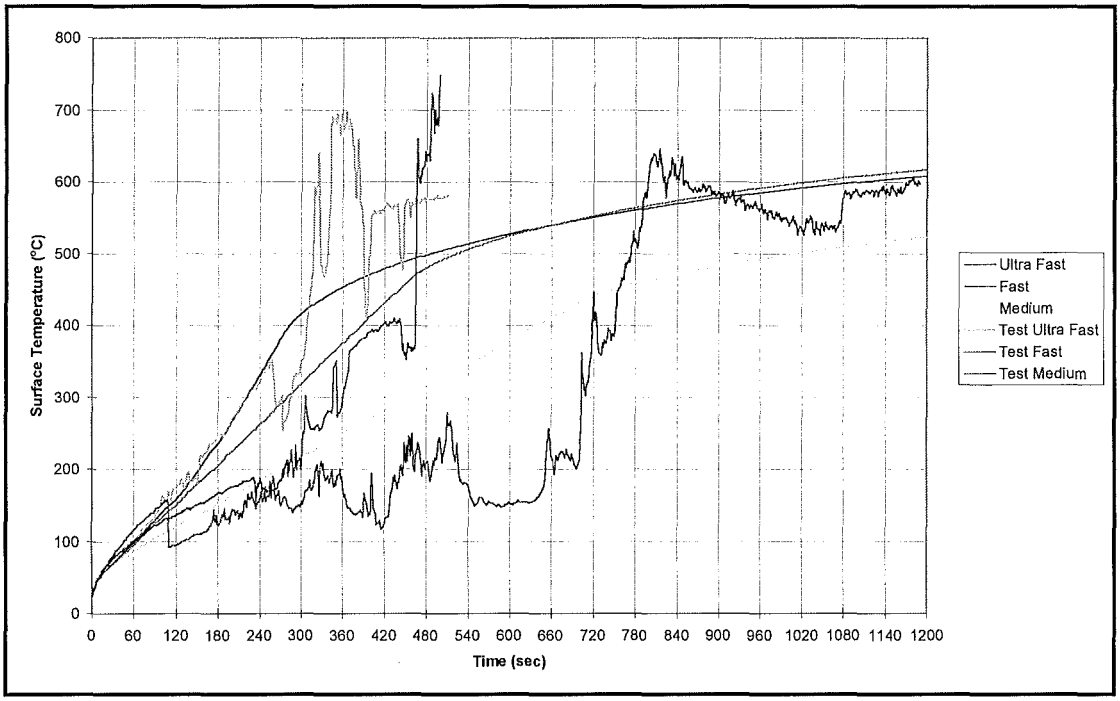


**Surface Temperature Profile and Model Output Temperature Curve Using Method Three to Calculate the Thermal Properties for Transient Flux Tests.**

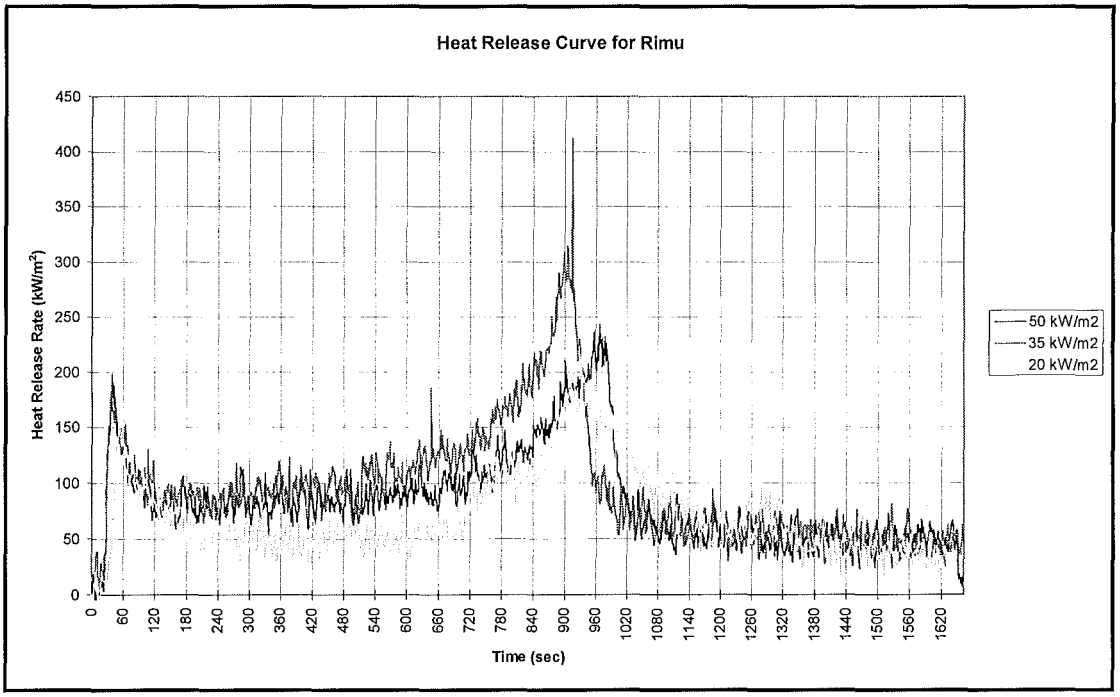


Heat Release Rate

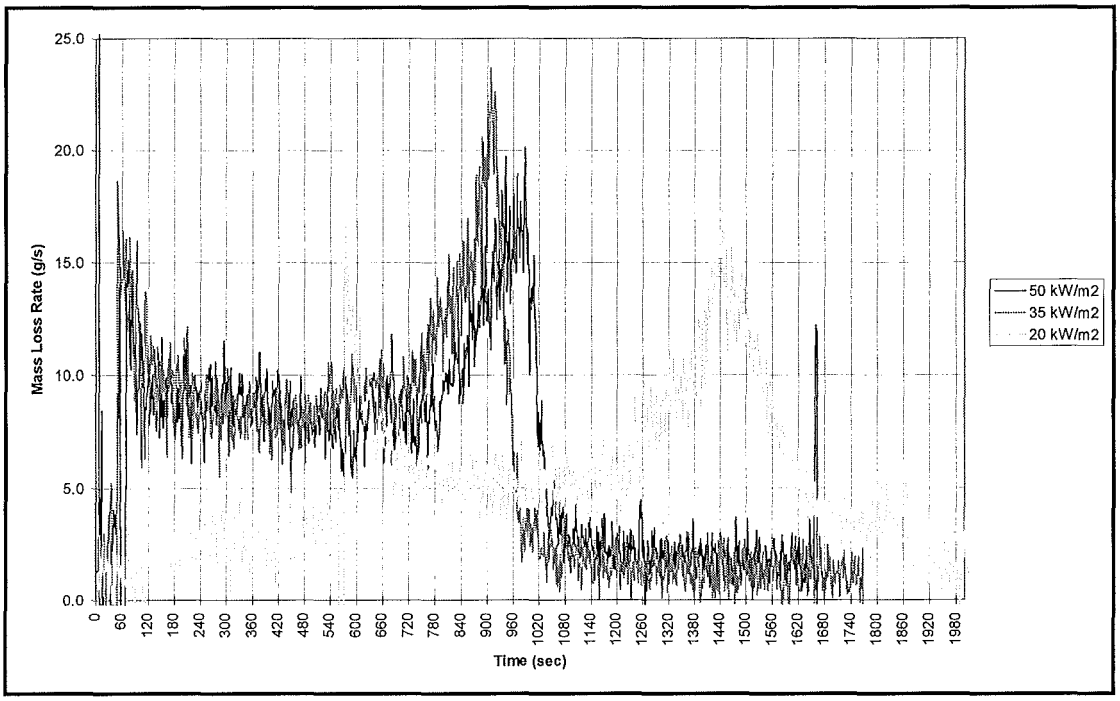


Mass Loss Rate

# Appendix B : Radiata Pine

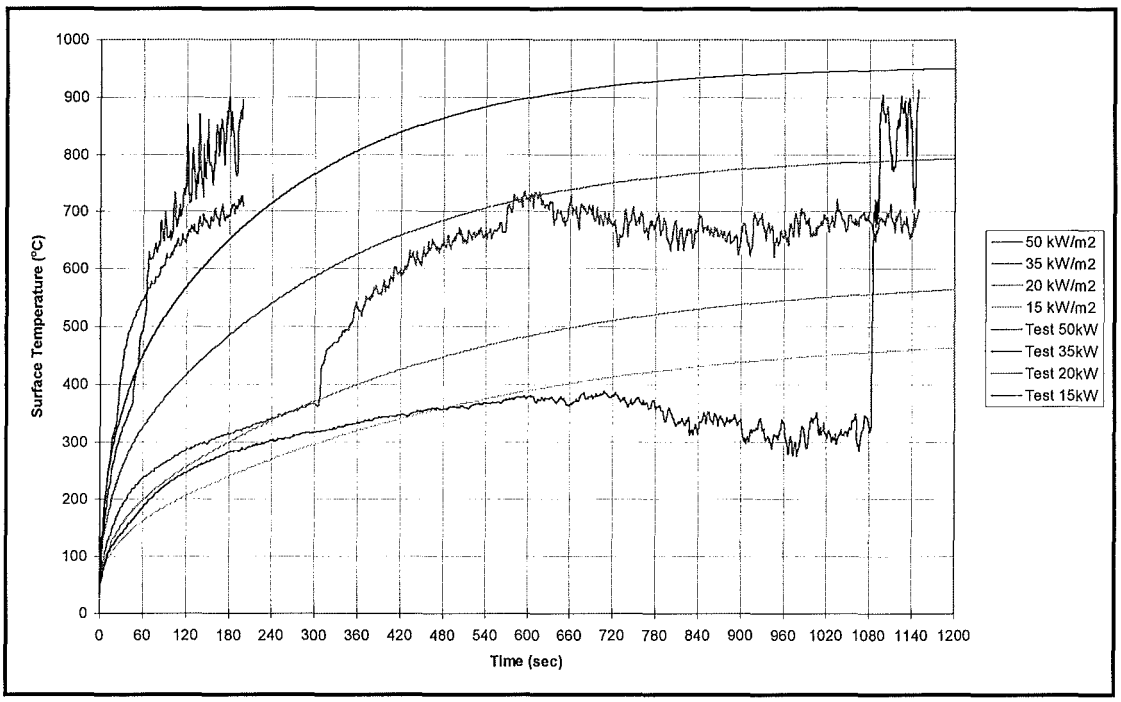


**Surface Temperature Profile and Model Output Temperature Curve Using Method One to Calculate the Thermal Properties for Constant Flux Tests.**

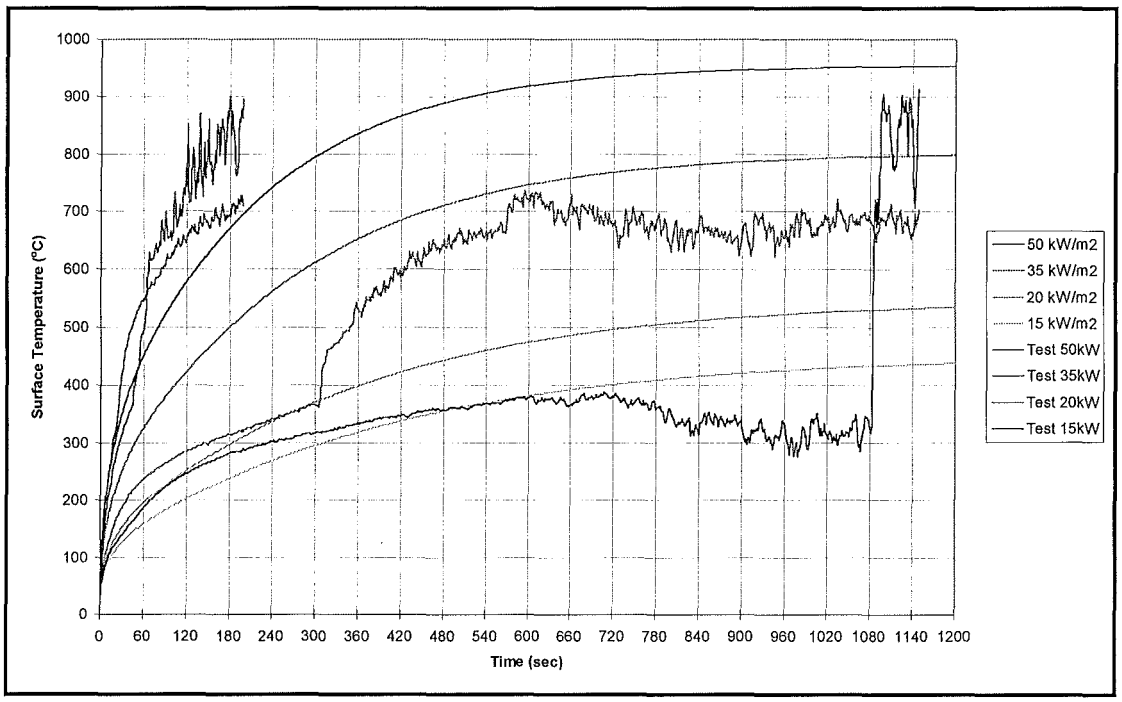


**Surface Temperature Profile and Model Output Temperature Curve Using Method Two to Calculate the Thermal Properties for Constant Flux Tests.**

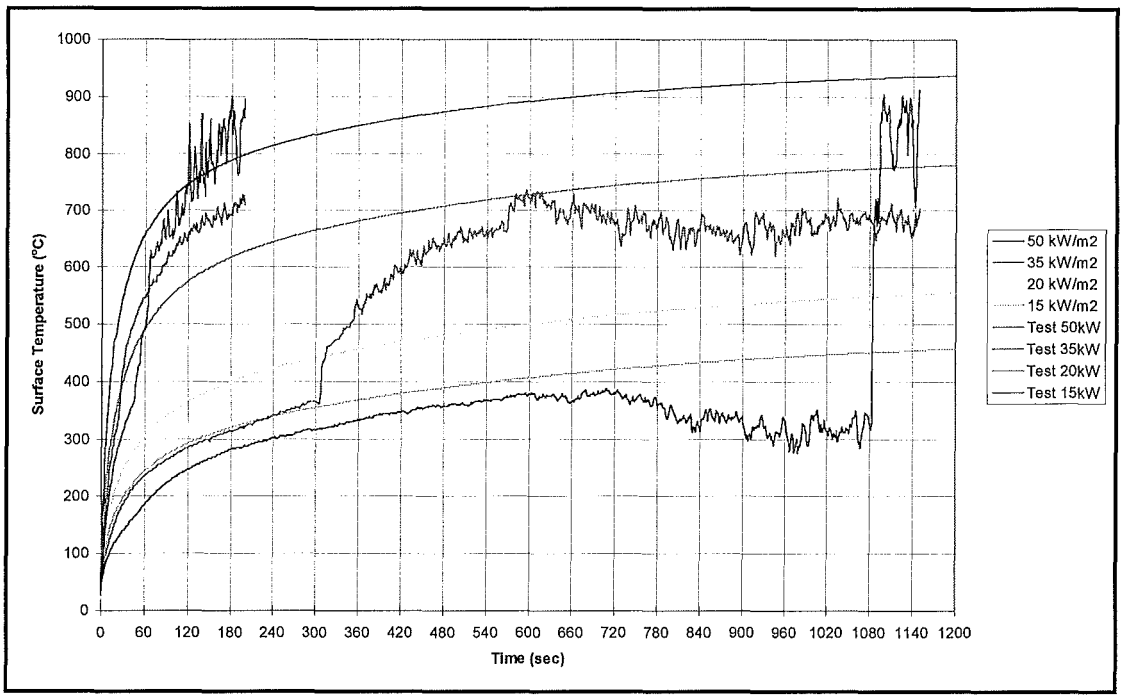


**Surface Temperature Profile and Model Output Temperature Curve Using Method Three to Calculate the Thermal Properties for Constant Flux Tests.**

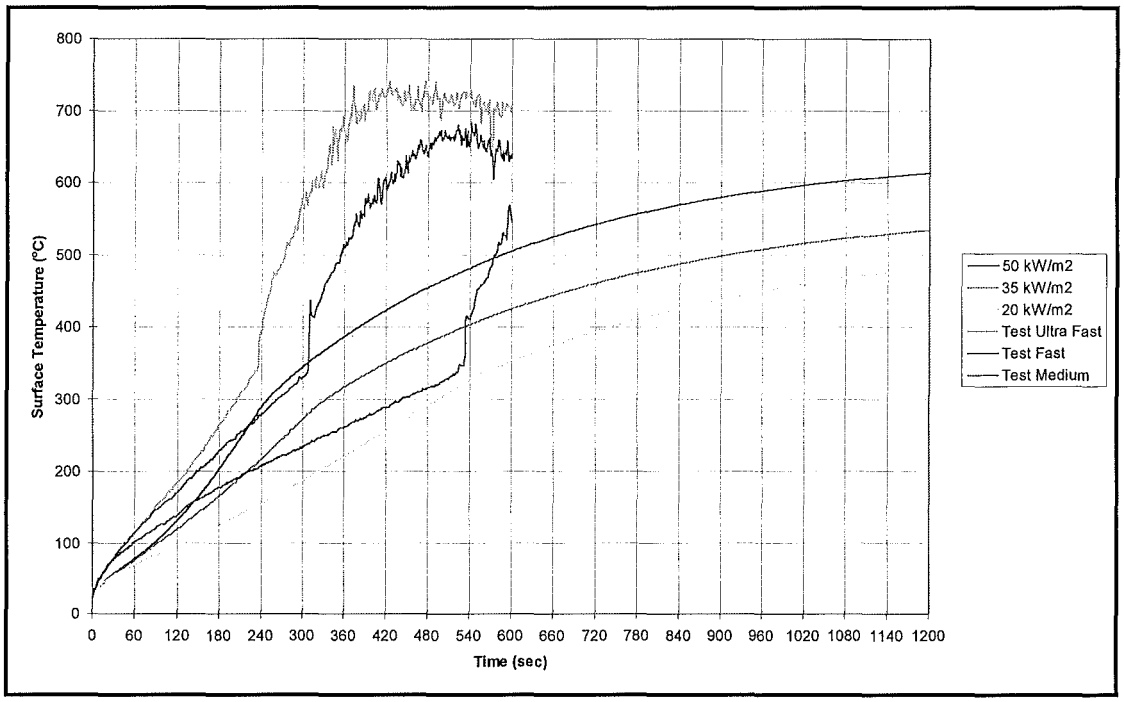


**Surface Temperature Profile and Model Output Temperature Curve Using Method One to Calculate the Thermal Properties for Transient Flux Tests.**

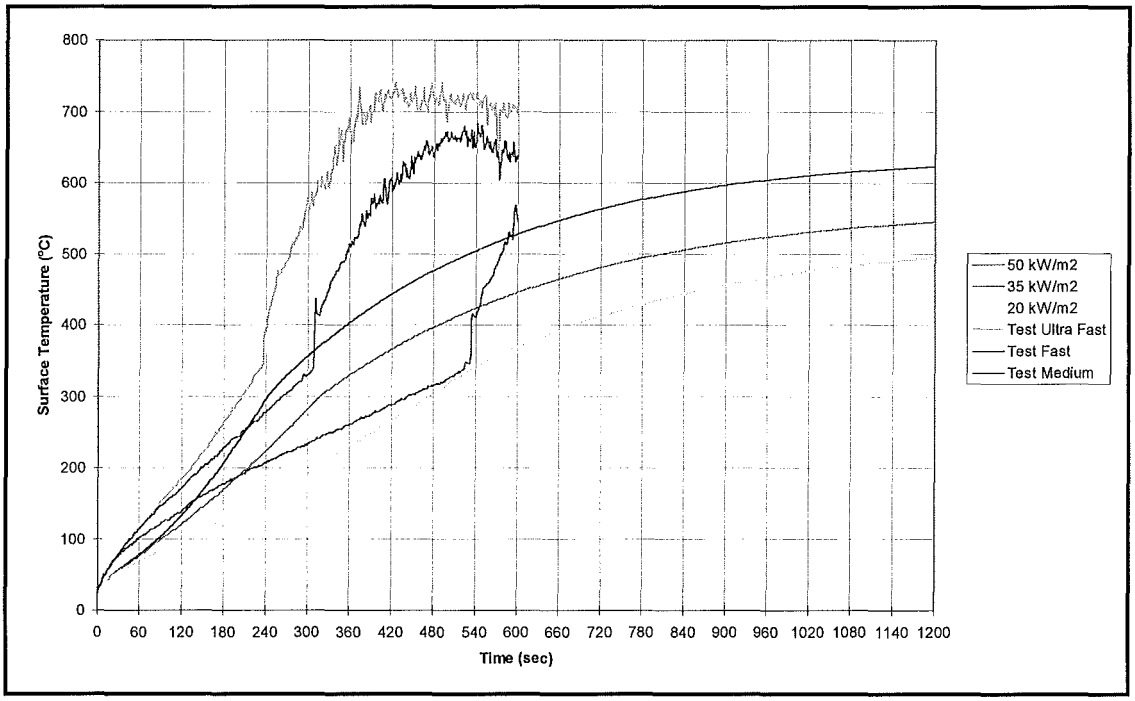


**Surface Temperature Profile and Model Output Temperature Curve Using Method Two to Calculate the Thermal Properties for Transient Flux Tests.**

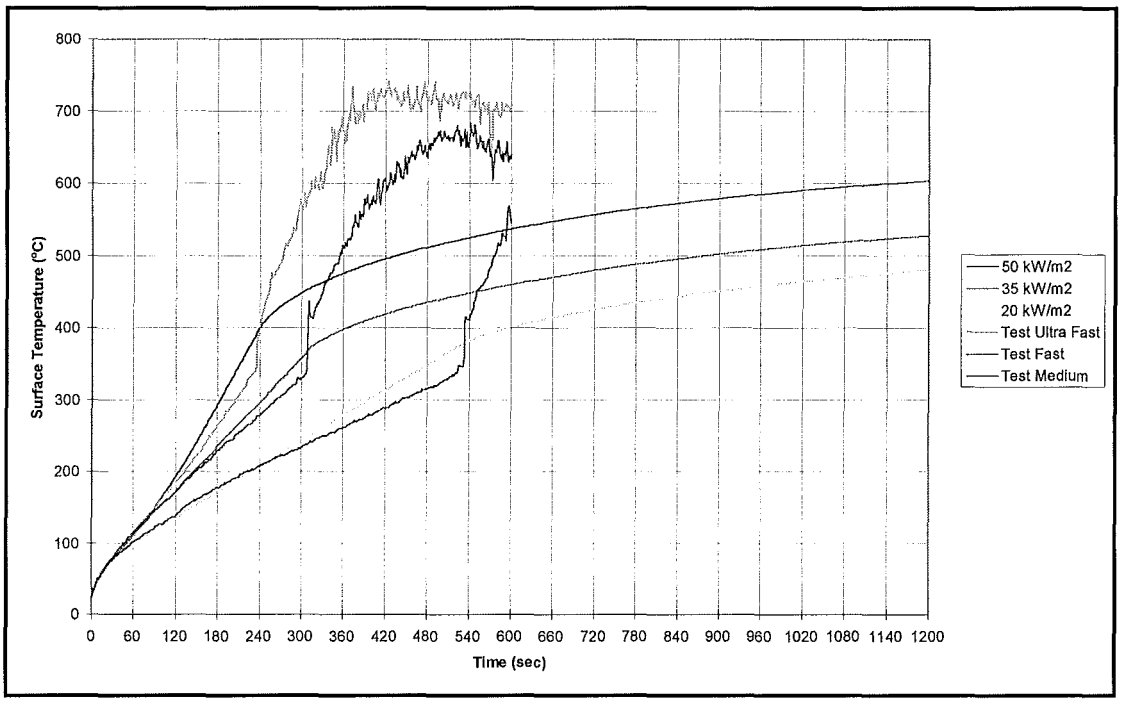


**Surface Temperature Profile and Model Output Temperature Curve Using Method Three to Calculate the Thermal Properties for Transient Flux Tests.**

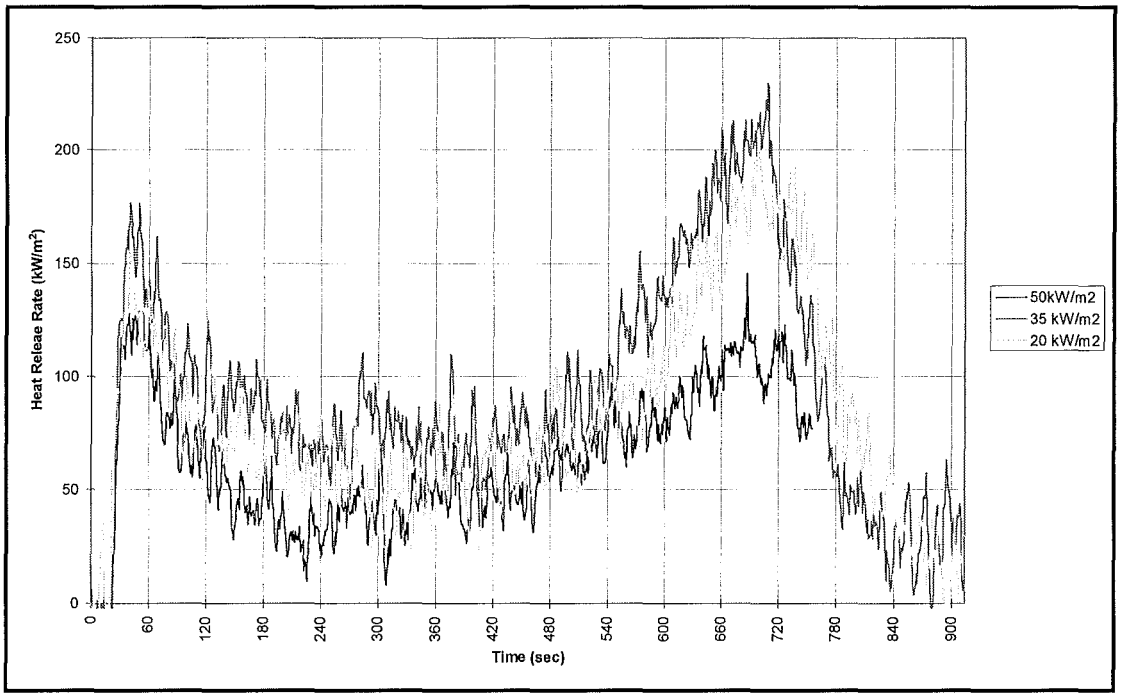


**Heat Release Rate**

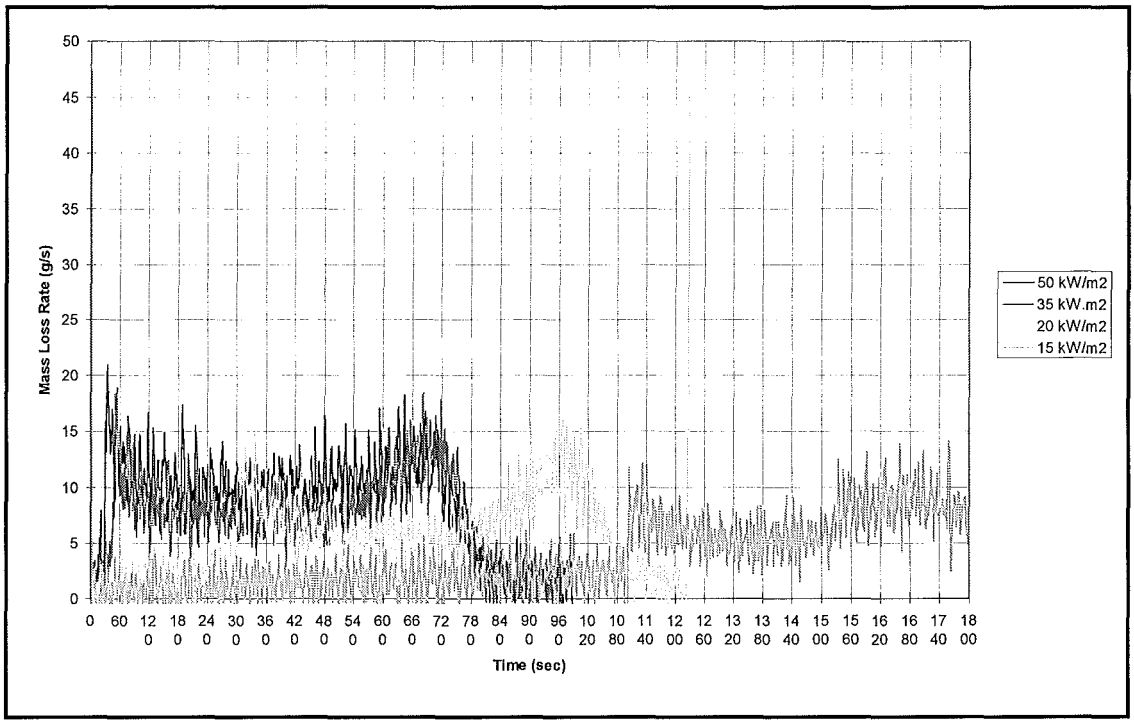


**Mass Loss Rate**

# Appendix C : Macracarpa

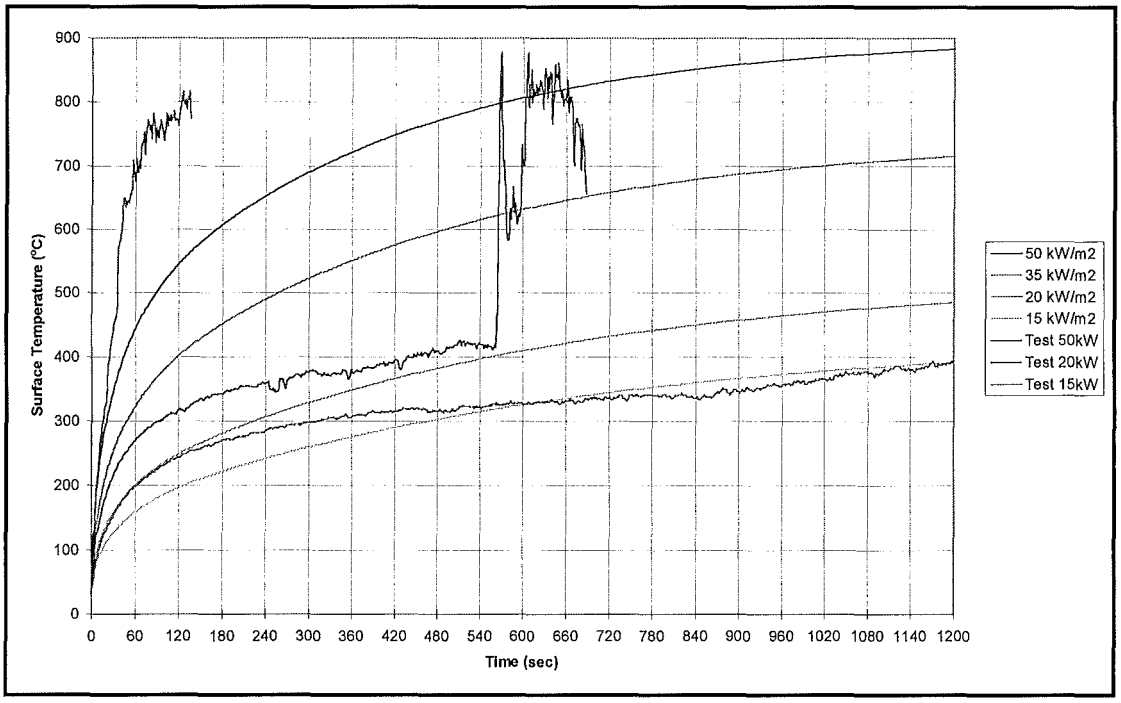


**Surface Temperature Profile and Model Output Temperature Curve Using Method One to Calculate the Thermal Properties for Constant Flux Tests.**

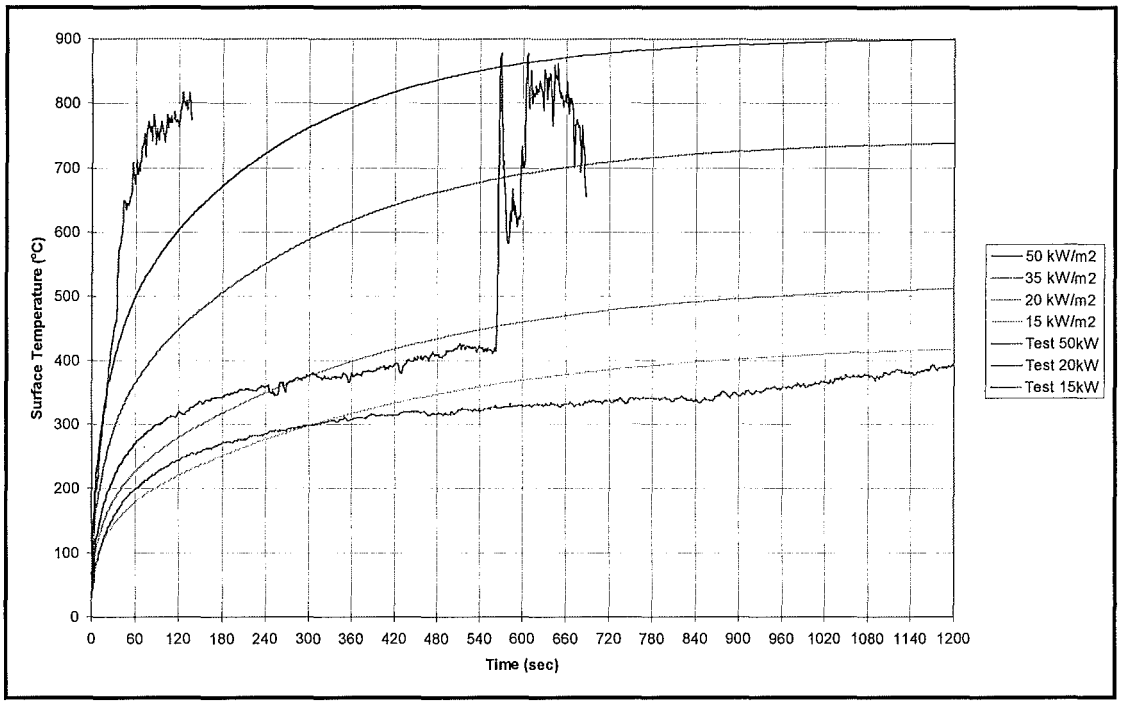


**Surface Temperature Profile and Model Output Temperature Curve Using Method Two to Calculate the Thermal Properties for Constant Flux Tests.**

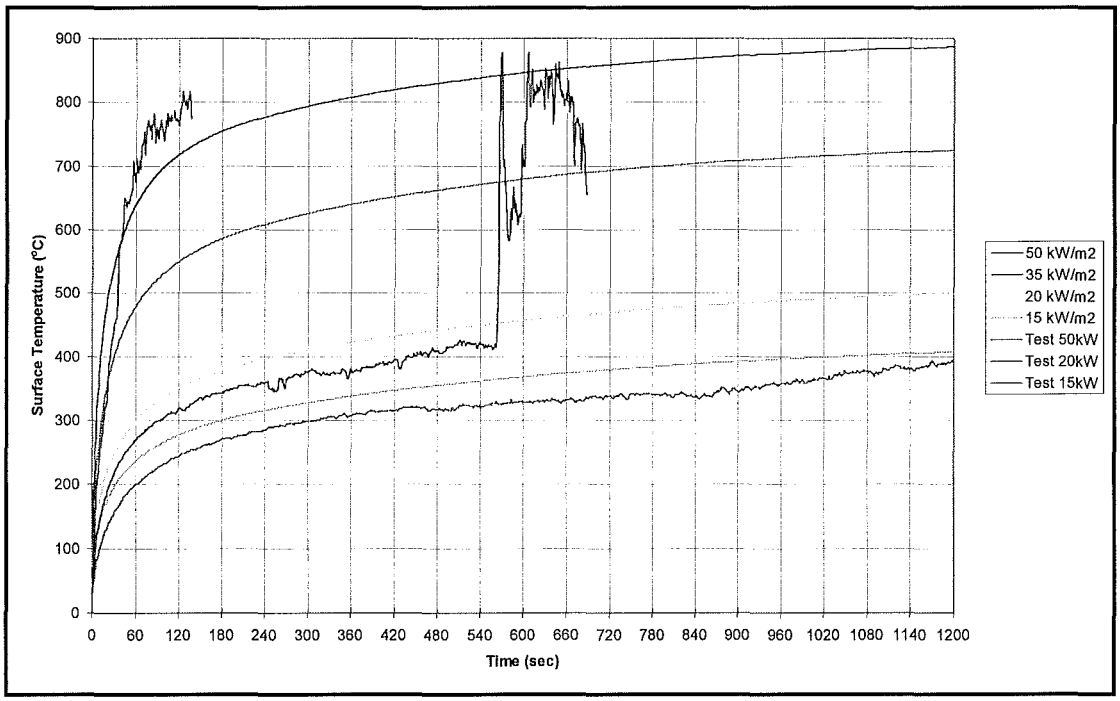


**Surface Temperature Profile and Model Output Temperature Curve Using Method Three to Calculate the Thermal Properties for Constant Flux Tests.**

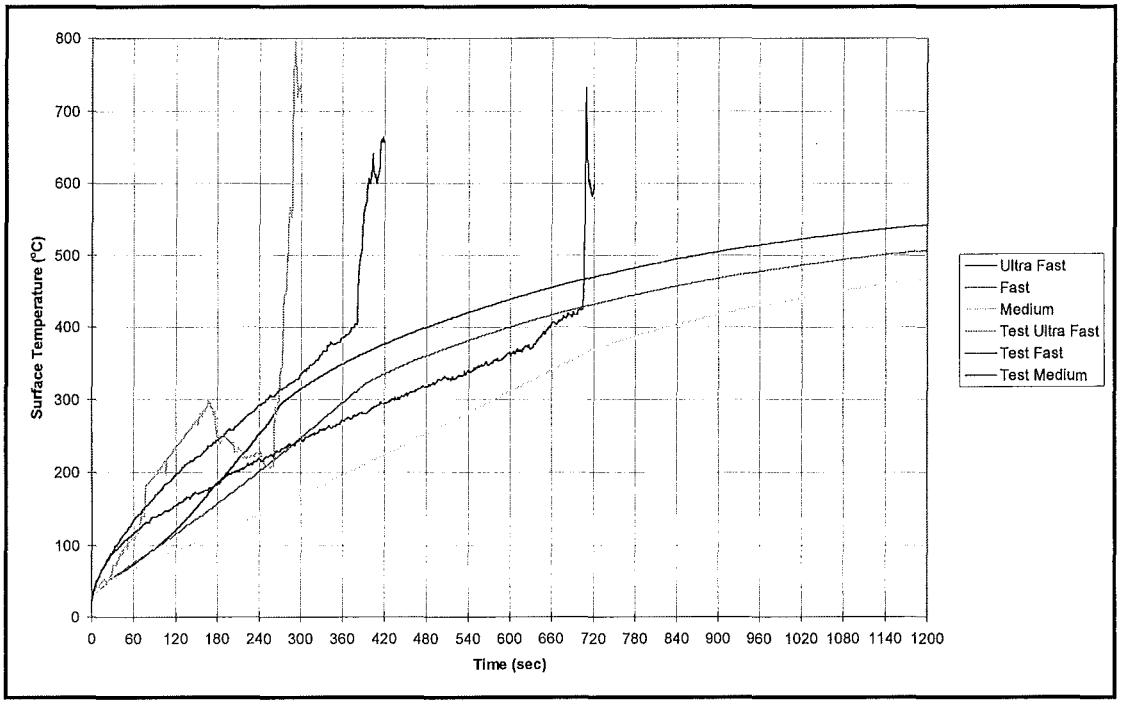


**Surface Temperature Profile and Model Output Temperature Curve Using Method One to Calculate the Thermal Properties for Transient Flux Tests.**

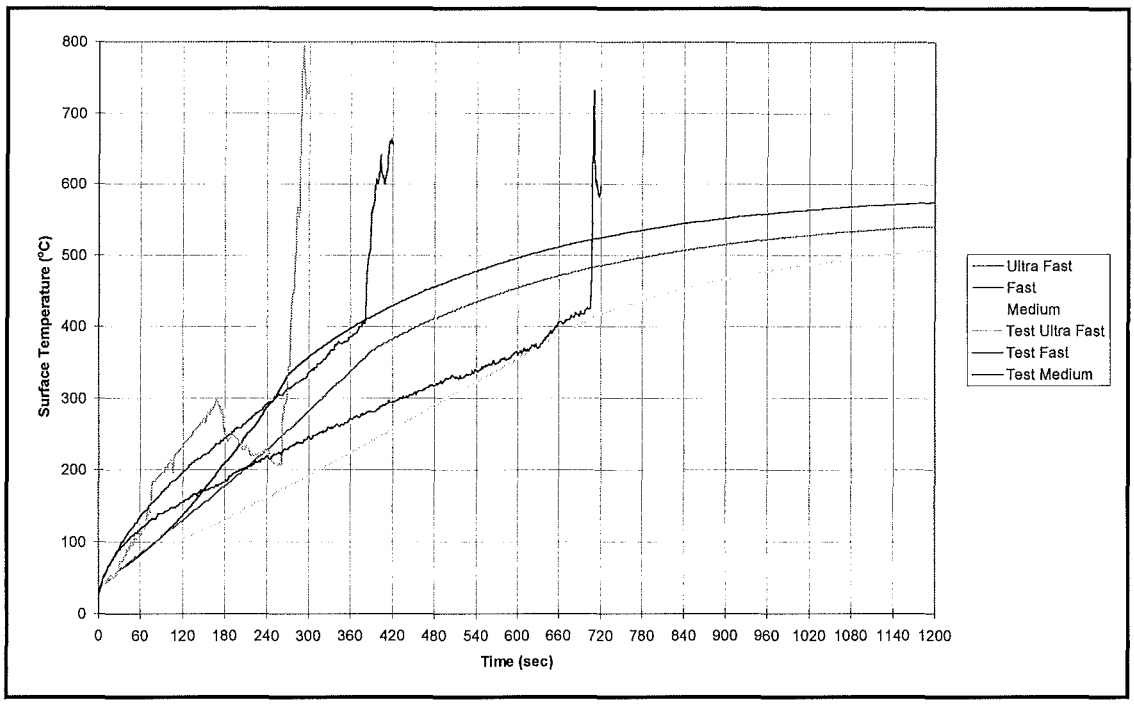


**Surface Temperature Profile and Model Output Temperature Curve Using Method Two to Calculate the Thermal Properties for Transient Flux Tests.**

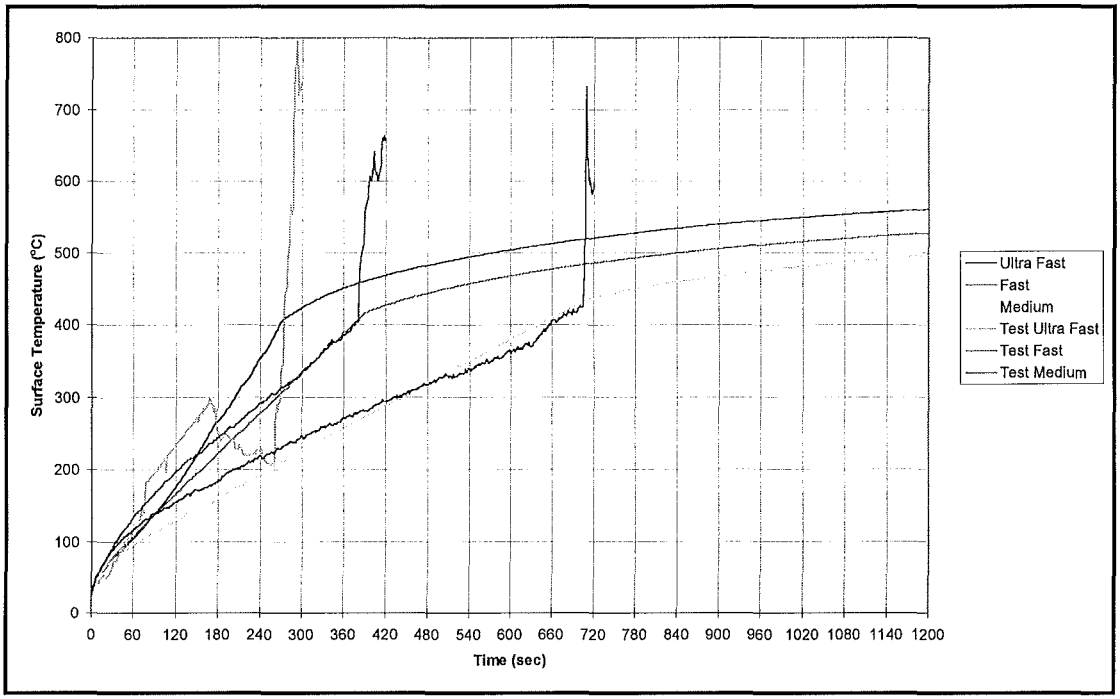


**Surface Temperature Profile and Model Output Temperature Curve Using Method Three to Calculate the Thermal Properties for Transient Flux Tests.**

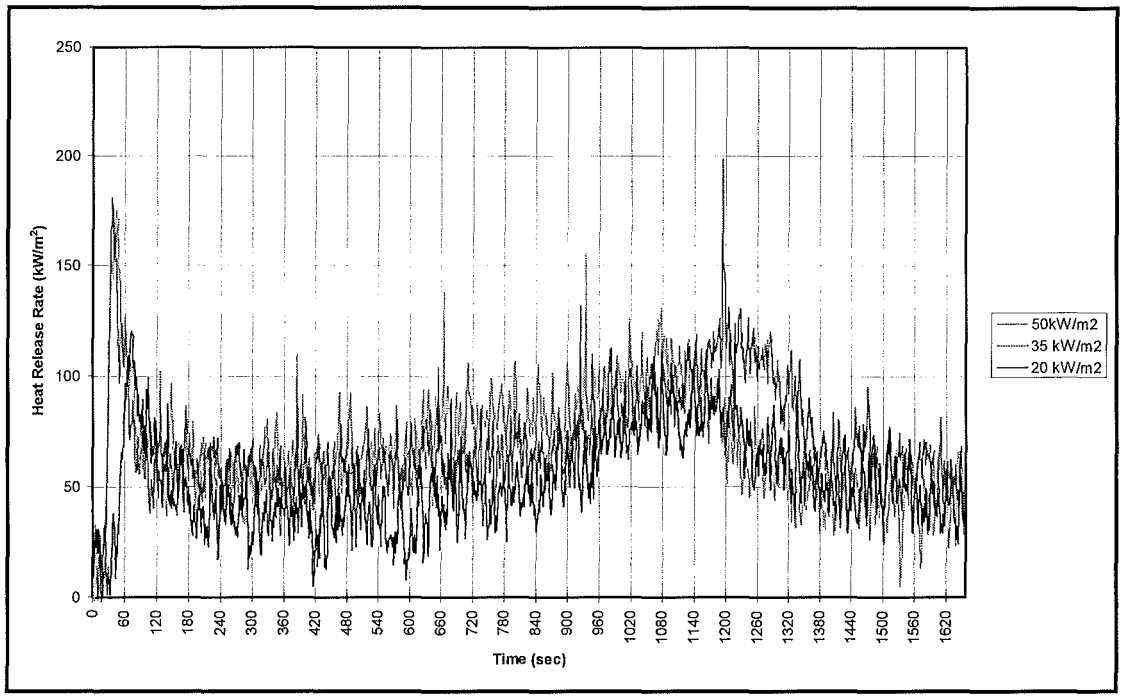


**Heat Release Rate**

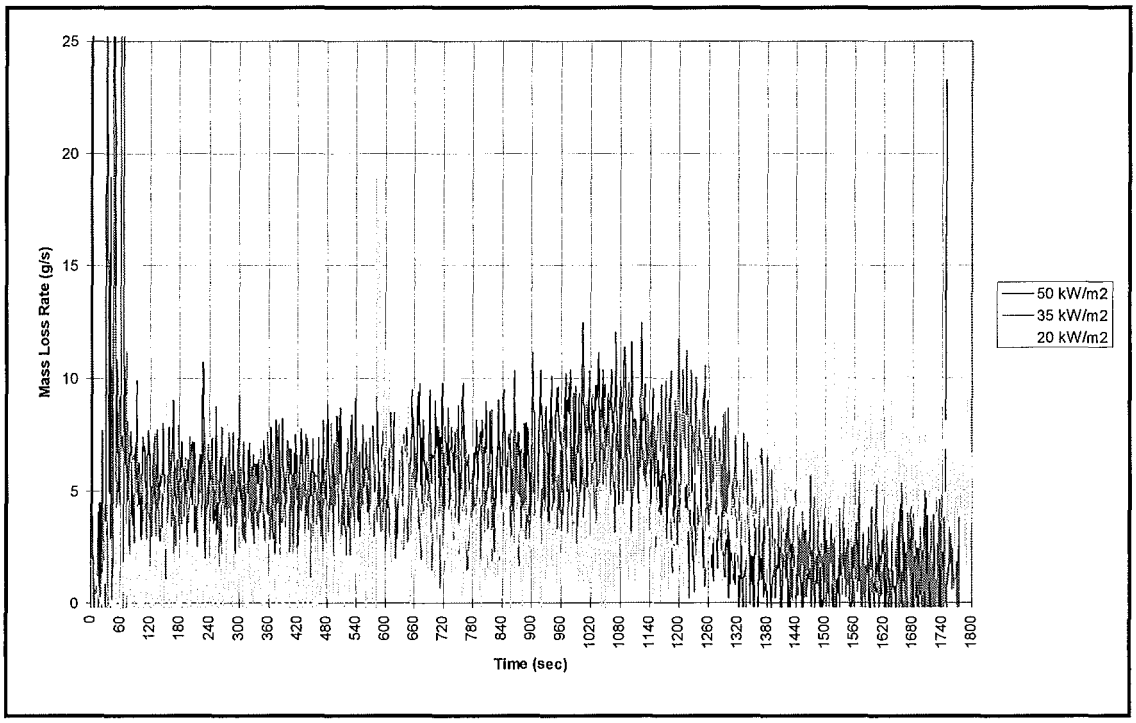


**Mass Loss Rate**

# Appendix D : Medium Density Fibreboard (MDF)

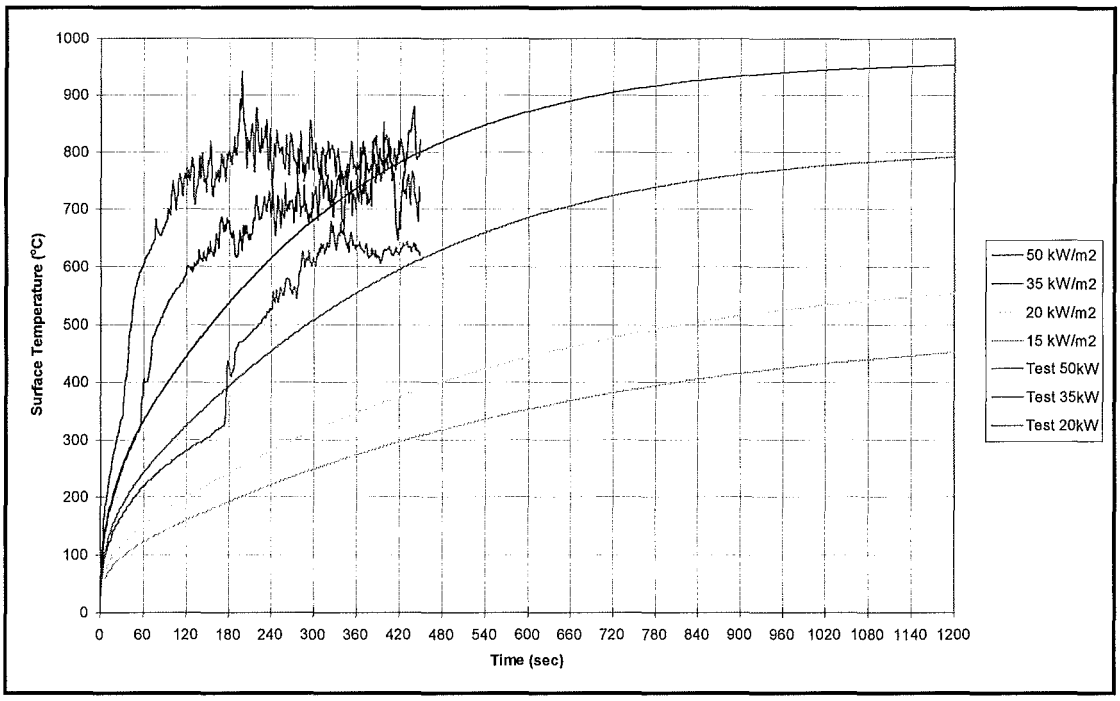


Surface Temperature Profile and Model Output Temperature Curve Using Method One to Calculate the Thermal Properties for Constant Flux Tests.

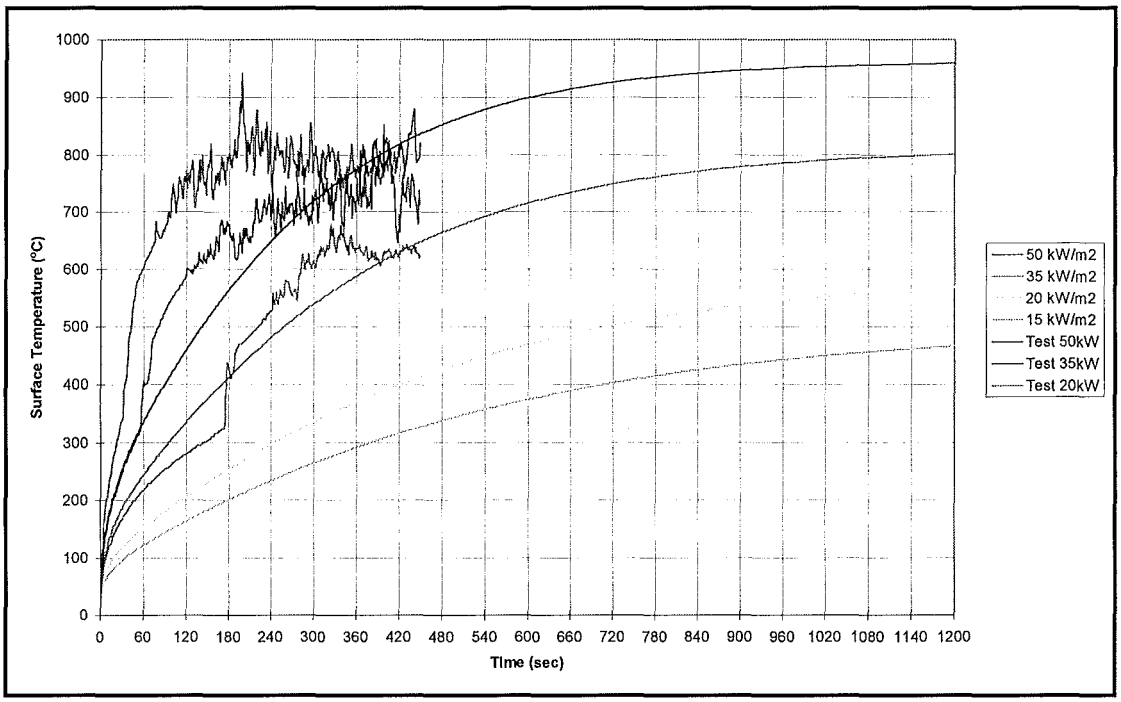


Surface Temperature Profile and Model Output Temperature Curve Using Method Two to Calculate the Thermal Properties for Constant Flux Tests.

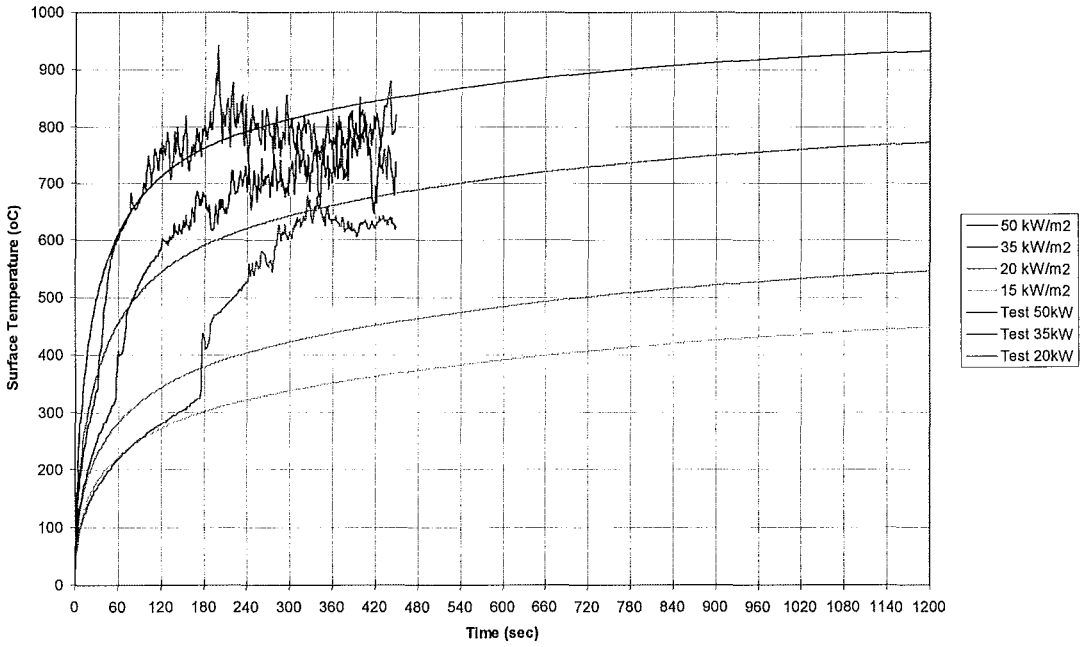


**Surface Temperature Profile and Model Output Temperature Curve Using Method Three to Calculate the Thermal Properties for Constant Flux Tests.**

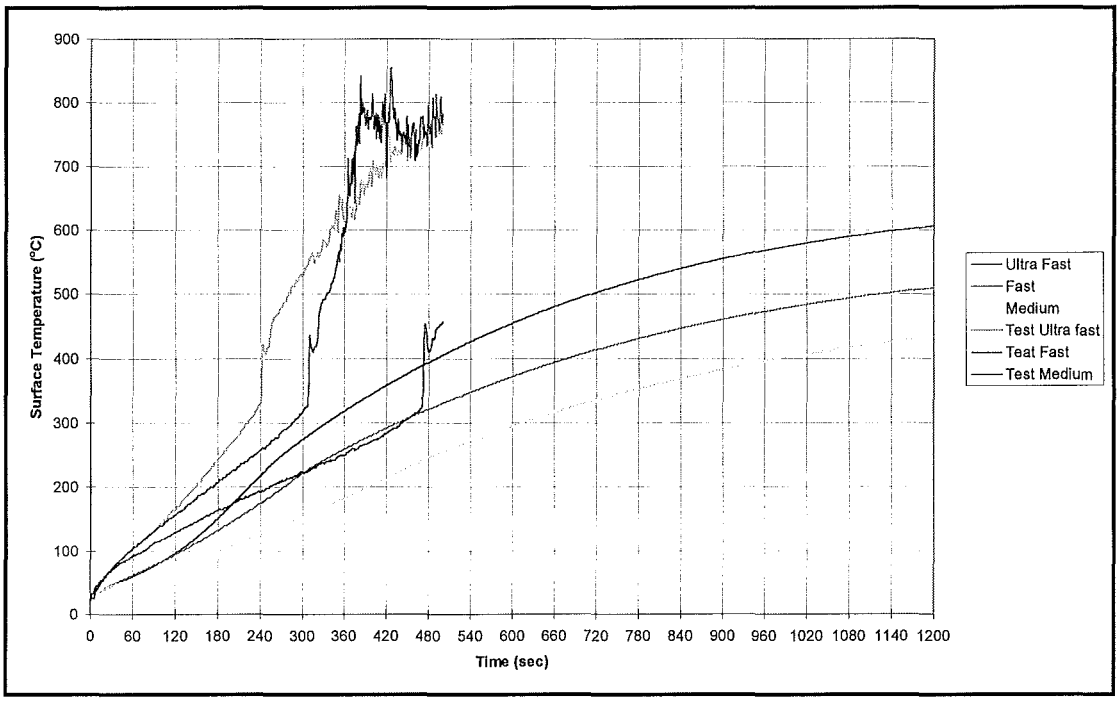


**Surface Temperature Profile and Model Output Temperature Curve Using Method One to Calculate the Thermal Properties for Transient Flux Tests.**

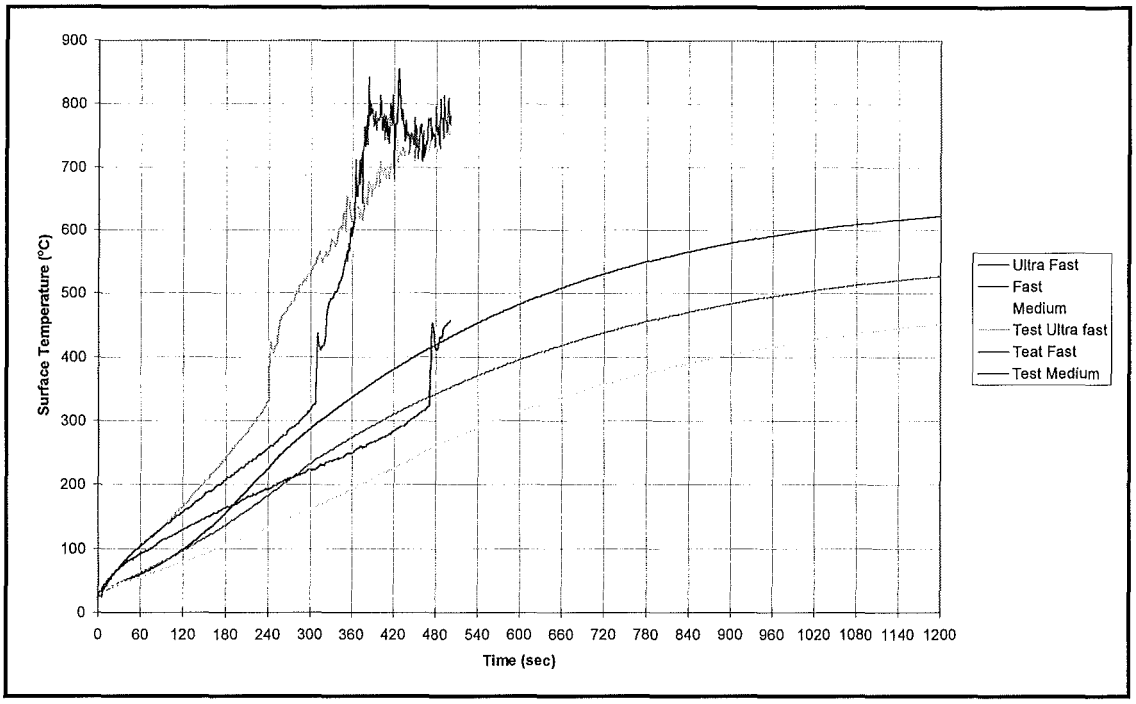


**Surface Temperature Profile and Model Output Temperature Curve Using Method Two to Calculate the Thermal Properties for Transient Flux Tests.**

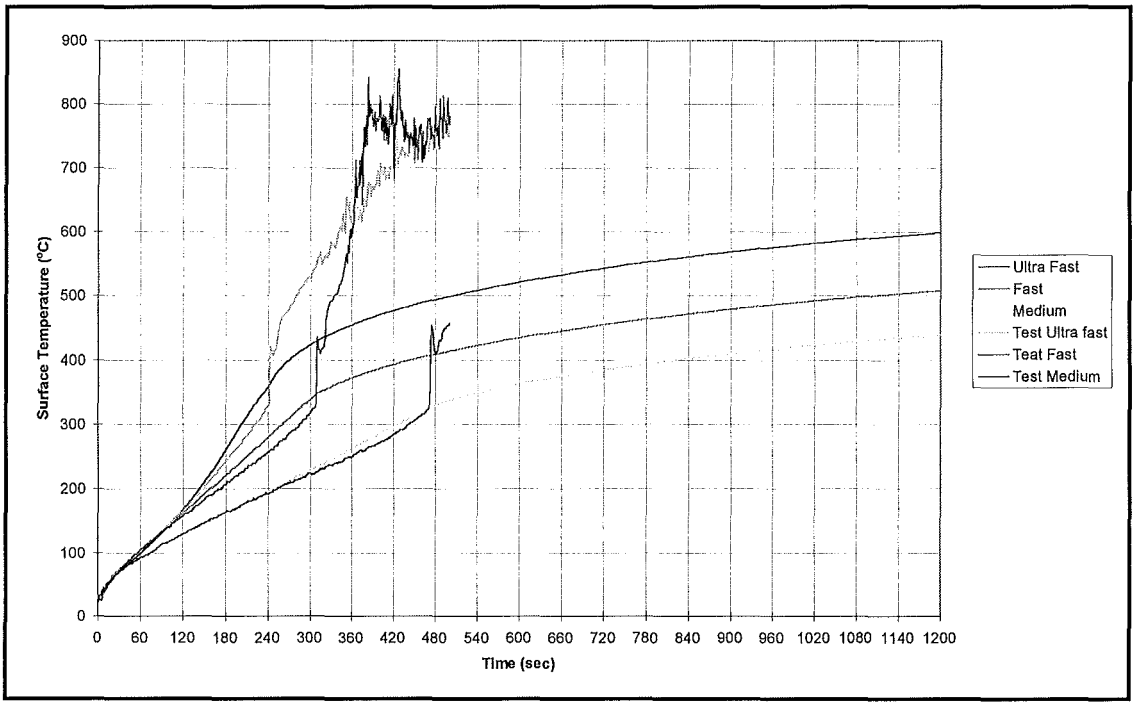


**Surface Temperature Profile and Model Output Temperature Curve Using Method Three to Calculate the Thermal Properties for Transient Flux Tests.**

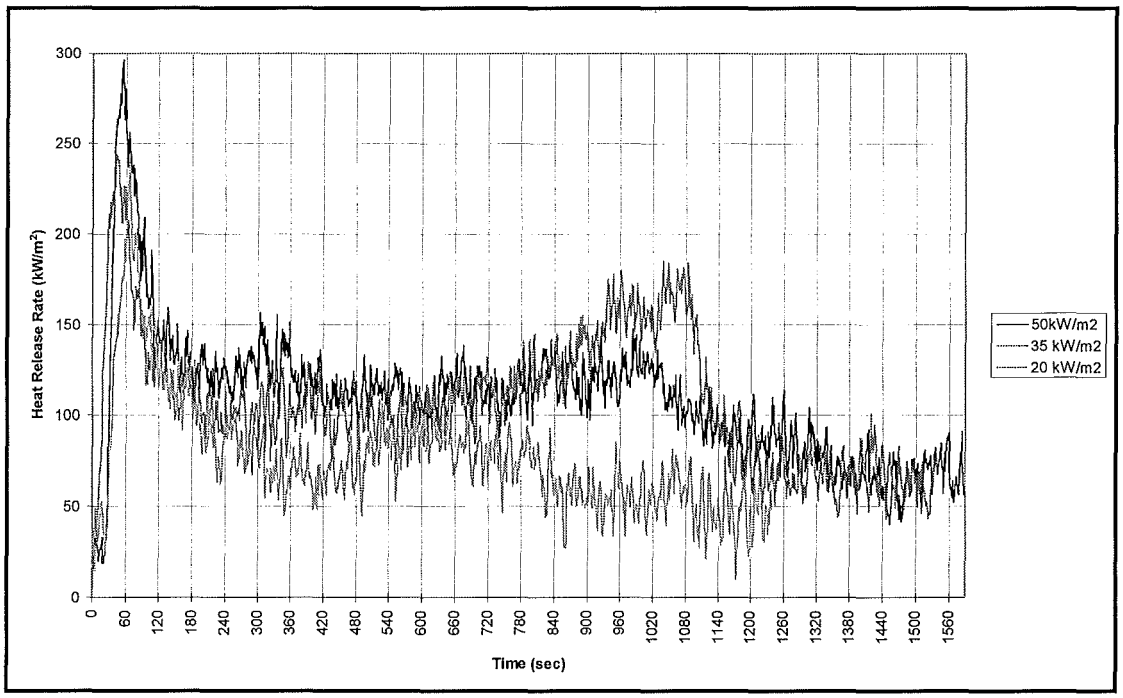


Heat Release Rate

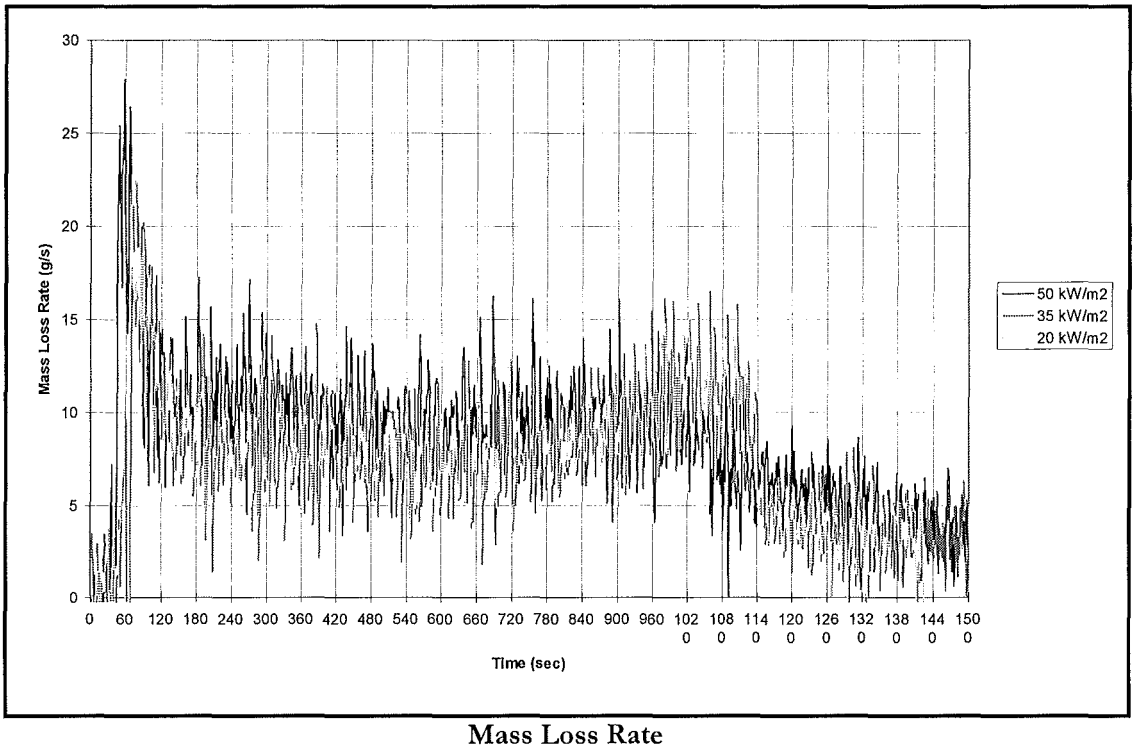


Mass Loss Rate

# Appendix E : Beech

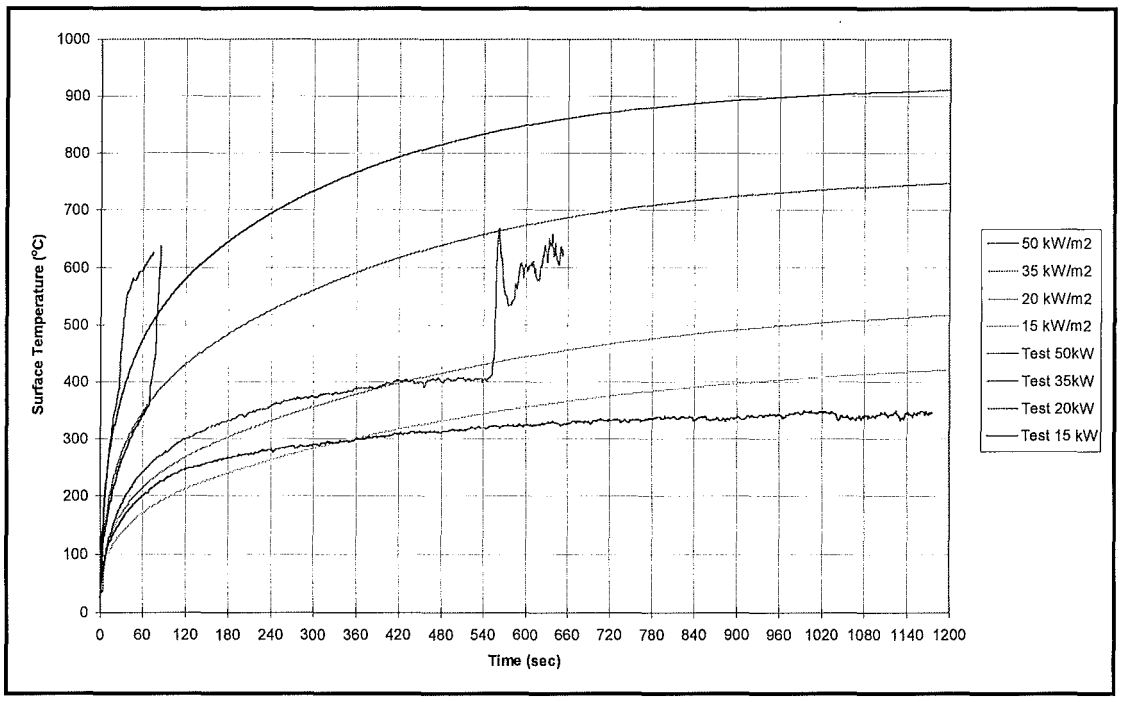


**Surface Temperature Profile and Model Output Temperature Curve Using Method One to Calculate the Thermal Properties for Constant Flux Tests.**

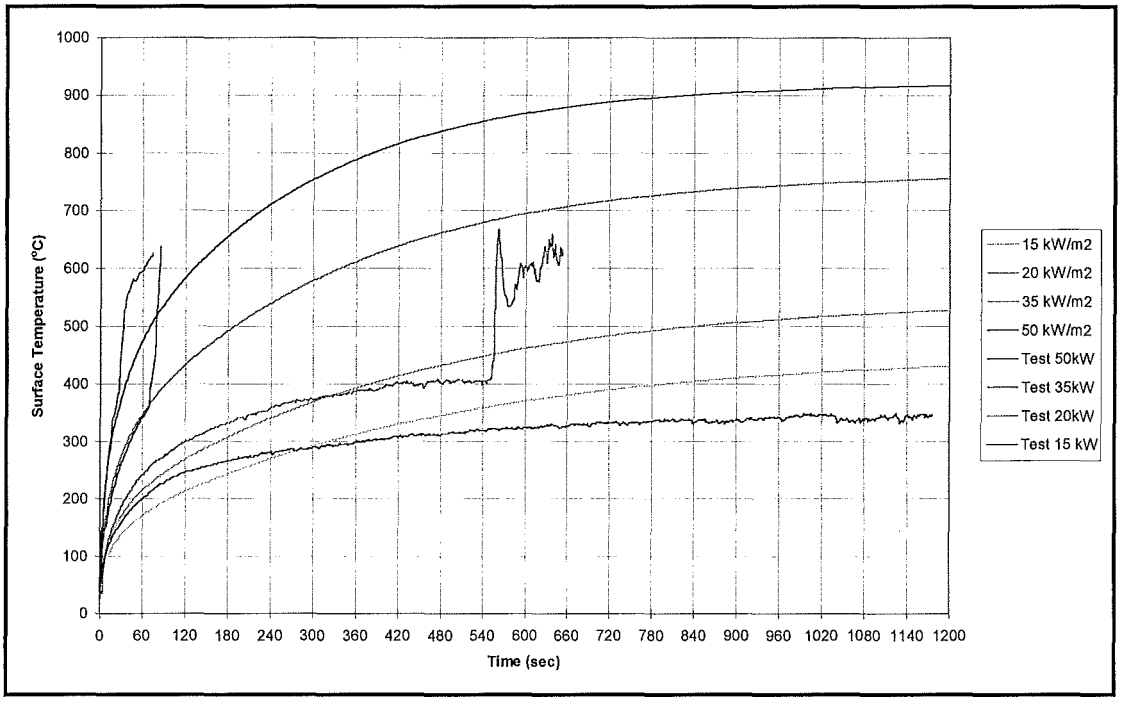


**Surface Temperature Profile and Model Output Temperature Curve Using Method Two to Calculate the Thermal Properties for Constant Flux Tests.**

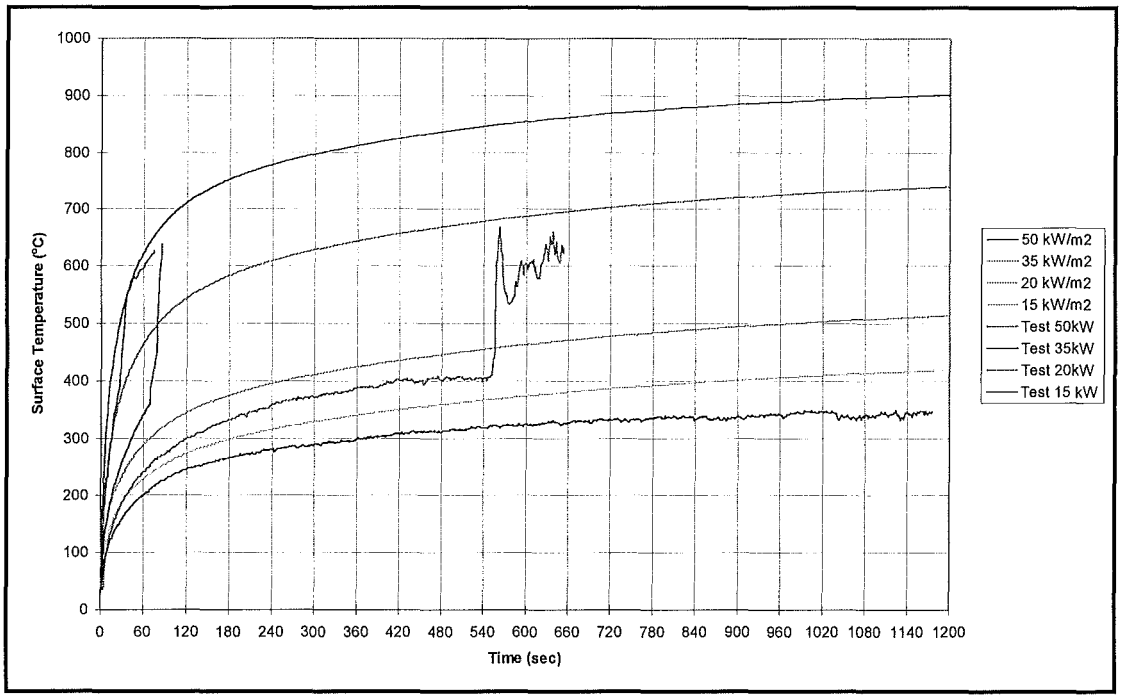


**Surface Temperature Profile and Model Output Temperature Curve Using Method Three to Calculate the Thermal Properties for Constant Flux Tests.**

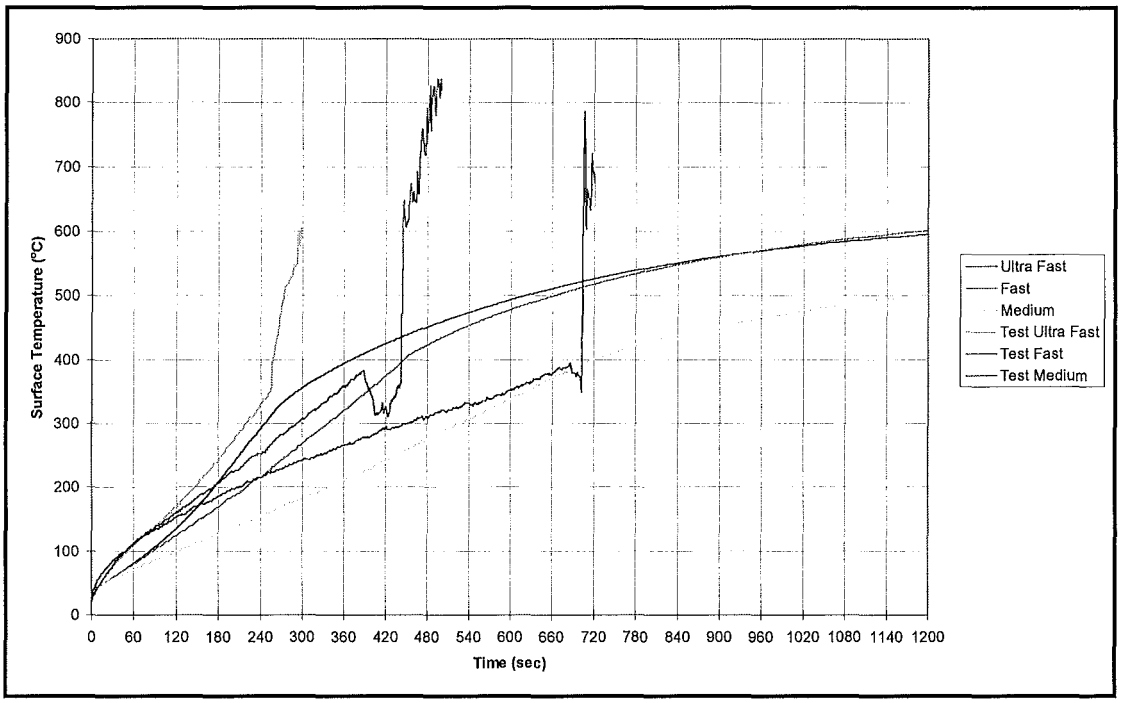


**Surface Temperature Profile and Model Output Temperature Curve Using Method One to Calculate the Thermal Properties for Transient Flux Tests.**

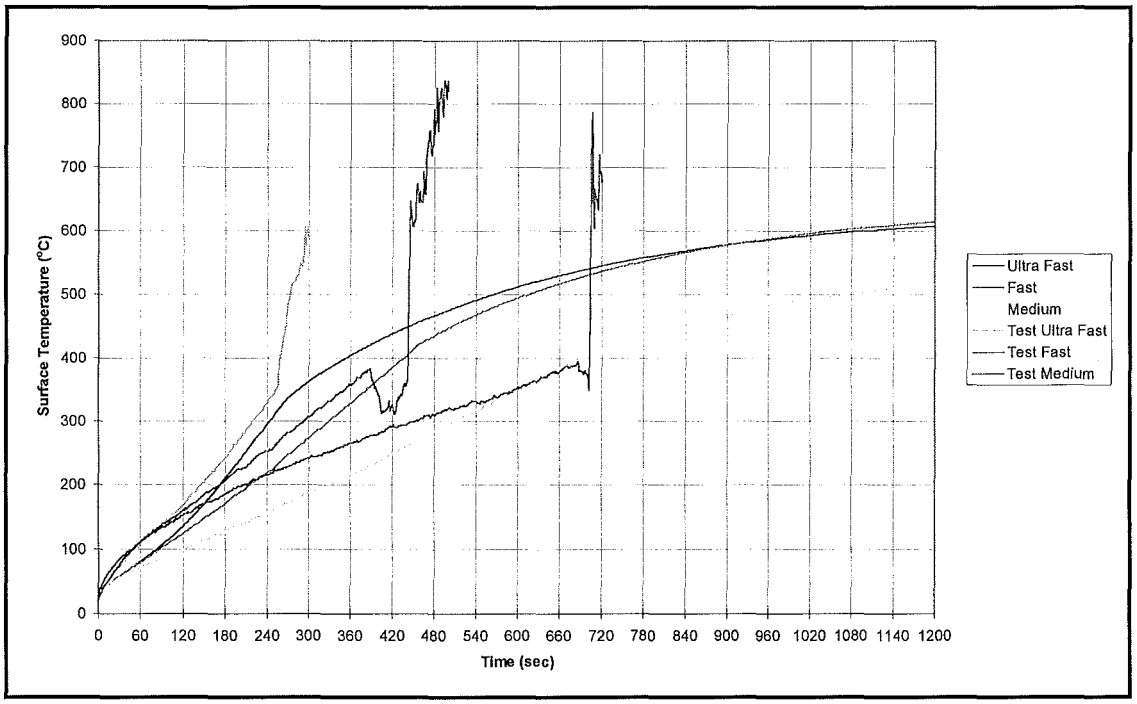


**Surface Temperature Profile and Model Output Temperature Curve Using Method Two to Calculate the Thermal Properties for Transient Flux Tests.**

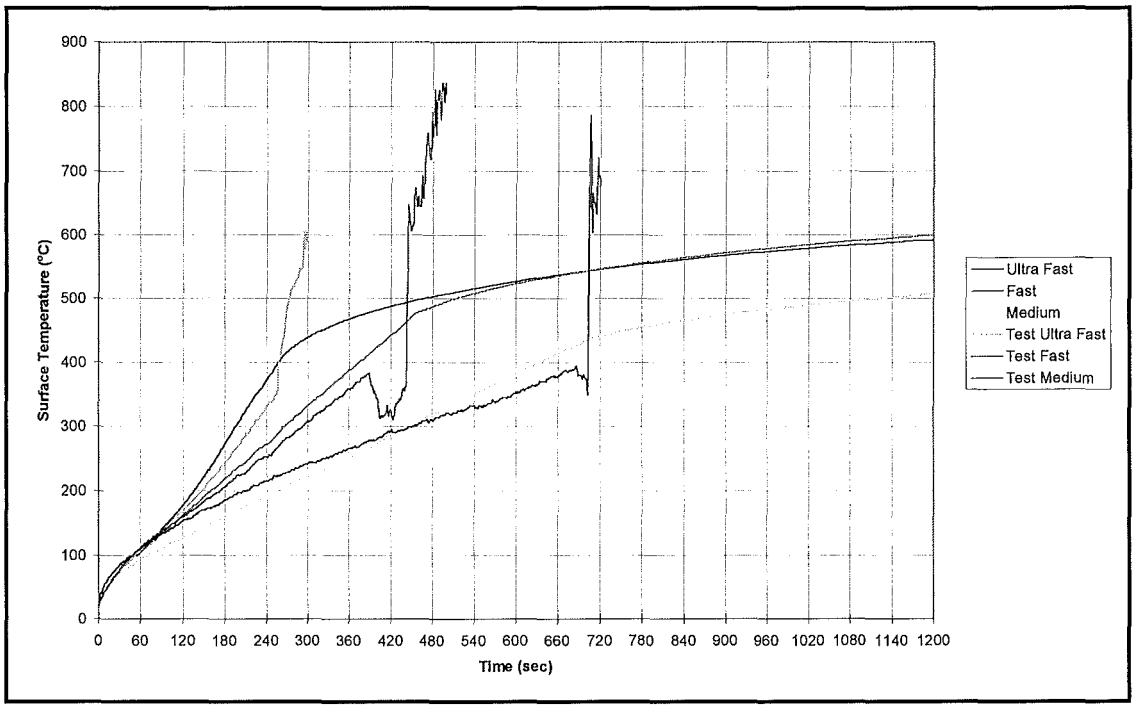


**Surface Temperature Profile and Model Output Temperature Curve Using Method Three to Calculate the Thermal Properties for Transient Flux Tests.**

# FIRE ENGINEERING RESEARCH REPORTS

| | | |
|---|---|---|
| 95/1 | **Full Residential Scale Backdraft** | **I B Bolliger** |
| 95/2 | **A Study of Full Scale Room Fire Experiments** | **P A Enright** |
| 95/3 | **Design of Load-bearing Light Steel Frame Walls for Fire Resistance** | **J T Gerlich** |
| 95/4 | **Full Scale Limited Ventilation Fire Experiments** | **D J Millar** |
| 95/5 | **An Analysis of Domestic Sprinkler Systems for Use in New Zealand** | **F Rahmanian** |
| 96/1 | **The Influence of Non-Uniform Electric Fields on Combustion Processes** | **M A Belsham** |
| 96/2 | **Mixing in Fire Induced Doorway Flows** | **J M Clements** |
| 96/3 | **Fire Design of Single Storey Industrial Buildings** | **B W Cosgrove** |
| 96/4 | **Modelling Smoke Flow Using Computational Fluid Dynamics** | **T N Kardos** |
| 96/5 | **Under-Ventilated Compartment Fires - A Precursor to Smoke Explosions** | **A R Parkes** |
| 96/6 | **An Investigation of the Effects of Sprinklers on Compartment Fires** | **M W Radford** |
| 97/1 | **Sprinkler Trade Off Clauses in the Approved Documents** | **G J Barnes** |
| 97/2 | **Risk Ranking of Buildings for Life Safety** | **J W Boyes** |
| 97/3 | **Improving the Waking Effectiveness of Fire Alarms in Residential Areas** | **T Grace** |
| 97/4 | **Study of Evacuation Movement through Different Building Components** | **P Holmberg** |
| 97/5 | **Domestic Fire Hazard in New Zealand** | **KDJ Irwin** |
| 97/6 | **An Appraisal of Existing Room-Corner Fire Models** | **D C Robertson** |
| 97/7 | **Fire Resistance of Light Timber Framed Walls and Floors** | **G C Thomas** |
| 97/8 | **Uncertainty Analysis of Zone Fire Models** | **A M Walker** |
| 97/9 | **New Zealand Building Regulations Five Years Later** | **T M Pastore** |
| 98/1 | **The Impact of Post-Earthquake Fire on the Built Urban Environment** | **R Botting** |
| 98/2 | **Full Scale Testing of Fire Suppression Agents on Unshielded Fires** | **M J Dunn** |
| 98/3 | **Full Scale Testing of Fire Suppression Agents on Shielded Fires** | **N Gravestock** |
| 98/4 | **Predicting Ignition Time Under Transient Heat Flux Using Results from Constant Flux Experiments** | **A Henderson** |
| 98/5 | **Comparison Studies of Zone and CFD Fire Simulations** | **A Lovatt** |
| 98/6 | **Bench Scale Test of Light Timber Frame Walls** | **P Olsson** |
| 98/7 | **Exploratory Salt Water Experiments of Balcony Spill Plume Using Laser Induced Fluorescence Technique** | **E Y Yii** |

School of Engineering
University of Canterbury
Private Bag 4800, Christchurch, New Zealand

Phone 643 364-2250
Fax 643 364-2758